Partial restoration of spin-isospin SU(4) symmetry and the one-quasiparticle random-phase approximation method in double-β decay

V. dos S. Ferreira, F. Krmpotić, C. A. Barbero, and A. R. Samana

Phys. Rev. C **96**, 044322 — Published 23 October 2017

DOI: 10.1103/PhysRevC.96.044322

Partial restoration of spin-isospin $SU(4)$ Symmetry and the One-QRPA method in Double Beta Decay

V. dos S. Ferreira[1,2], F. Krmpotić[3], C.A. Barbero [3] and A. R. Samana[2]
[1] *Instituto de Física, Universidade do Estado do Rio de Janeiro, CEP 20550-900, Rio de Janeiro-RJ, Brazil*
[2] *Departamento de Ciências Exactas e Tecnológicas, Universidade Estadual de Santa Cruz, CEP 45662-000 Ilhéus, Bahia-BA, Brazil and*
[3] *Instituto de Física La Plata, CONICET, Universidad Nacional de La Plata, 1900 La Plata, Argentina,*

The one-QRPA method is used to describe simultaneously both double decay beta modes, giving special attention to the partial restoration of spin-isospin $SU(4)$ symmetry. To implement this restoration and to fix the model parameters, we resort to the energetics of Gamow-Teller resonances and to the minima of the single β^+-decay strengths. This makes the theory predictive regarding the $\beta\beta_{2\nu}$-decay, producing the 2ν moments in ^{48}Ca, ^{76}Ge, ^{82}Se, ^{96}Zr, ^{100}Mo, ^{128,130}Te, and ^{150}Nd, that are of the same order of magnitude as the experimental ones; however, the agreement with $\beta\beta_{2\nu}$ data is only modest. To include contributions coming from induced nuclear weak currents, we extend the $\beta\beta_{0\nu}$-decay formalism employed previously in C. Barbero *et al.*, Nuc. Phys. **A628**, 170 (1998), which is based on the Fourier-Bessel expansion. The numerical results for the $\beta\beta_{0\nu}$ moments in the above mentioned nuclei are similar to those obtained in other theoretical studies although smaller on average by $\sim 40\%$. We attribute this difference basically to the one-QRPA-method, employed here for the first time, instead of the currently used two-QRPA-method. The difference is partially due also to the way of carrying out the restoration of the spin-isospin symmetry. It is hard to say which is the best way to make this restoration, since the $\beta\beta_{0\nu}$ moments are not experimentally measurable. The recipe proposed here is based on physically robust arguments. The numerical uncertainties in the $\beta\beta$ moments, related with: i) their strong dependence on the residual interaction in the particle-particle channel when evaluated within the QRPA, and ii) lack of proper knowledge of single-particle energies, have been quantified. It is concluded that the partial restoration of the $SU(4)$ symmetry, generated by the residual interaction, is crucial in the description of the $\beta\beta$-decays, regardless of the nuclear model used.

I. INTRODUCTION

Due to the nuclear pairing force, there exists in nature about 50 "anomalous" nuclear structure systems where the odd-odd isobar, within the isobaric triplet (N, Z), $(N-1, Z+1)$, $(N-2, Z+2)$, has a higher mass than the even-even neighbors. As a consequence, the single β-decay is energetically forbidden and $\beta\beta$-decay turns out to be the only possible mode of disintegration. This is a second-order weak process whose electromagnetic analogies are the atomic Raman scattering and nuclear $\gamma\gamma$-decay [1]. It is the slowest physical process observed so far, and can be used to learn about neutrino physics, provided we know how to deal with the nuclear structure.

The usual modes of $\beta\beta$ disintegrations are: (i) the two-neutrino double beta ($\beta\beta_{2\nu}$) decay, that can occur by two successive β decays, passing through the intermediate virtual states of the $(N-1, Z+1)$ nucleus, and (ii) the neutrinoless $\beta\beta$ ($\beta\beta_{0\nu}$) decay, where there are no neutrinos in the final state. There is consensus in the scientific community that we shall not understand the $\beta\beta_{0\nu}$-decay unless we understand the $\beta\beta_{2\nu}$-decay. Our goal is to describe the two $\beta\beta$-decay modes consistently.

The neutrino massiveness was definitively established at the end of the 20th century through experimental observation of neutrino oscillations [2]. Nevertheless, despite this great progress, some fundamental properties are still unknown in neutrino physics, such as the Dirac or Majorana nature of neutrinos (whether they are their own antiparticle), or the absolute neutrino mass-scale and hierarchy. The first question would be answered with the detection of the $\beta\beta_{0\nu}$-decay. The atomic nuclei are used as the detectors of the elusive neutrinos and the next generation of experiments for many different nuclei is searching for this rare decay mode, including ^{48}Ca, ^{76}Ge, ^{100}Mo, ^{116}Cd,^{128,130}Te, ^{124,126,134}Xe, ^{136}Ce, ^{150}Nd, and ^{160}Gd. A summary of the experiments with the above nuclei is well explained in recent reviews, such as in Barabash [3], or Tosi [4].

A realistic quantum many-body system is generally characterized by a generic microscopic Hamiltonian, which is accessible only through approximate methods. In this regard, the mean-field theories commonly serve as an appropriate starting point but, unfortunately, they often violate the symmetries of the Hamiltonian. Such is the case for conventional BCS theory, which is an excellent zero-order approximation. However, it violates both the conservation of particle number and the spin-isospin $SU(4)$ symmetry. The first of these disadvantages does not play a very important role, but the second is crucial in the description of the $\beta\beta$-decay [1]. There is a general

[1] As a matter of fact, a long time ago Bohr and Mottelson pointed out [5]: "The supermultiplet symmetry has approximate validity for the light nuclei spectra, but it is badly broken in heavier nuclei as a consequence of the strong spin-orbit coupling, which leads to the (jj) coupling. The correlations responsible for the

consensus regarding this issue that: i) the $SU(4)$ symmetry is to be restored by the residual interaction, and ii) that this restoration must not be complete as this would inhibit both $\beta\beta$-decays [8]. Therefore, we speak of Partial $SU(4)$ Symmetry Restoration (PSU4SR). The question is: how to do it in a proper way? Here, we make an attempt to answer this question.

The symmetries broken by the BCS are restored by the residual interaction via the Quasiparticle Random-Phase Approximation (QRPA) and, in recent years, significant attention has been devoted to the restoration of the isospin symmetry in the evaluation of the $\beta\beta$-decay nuclear moments (NM) within this framework [9–11]. This was accomplished by separating the renormalization parameter g_{pp} of the particle-particle proton-neutron interaction into isovector $g_{pp}^{T=1}$, and isoscalar $g_{pp}^{T=0}$ parts, and by choosing the first one to be essentially equal to the average pairing constant. In this way, the requirement that the Fermi (F) $\beta\beta_{2\nu}$ matrix element $M_F^{2\nu}$ vanishes is fulfilled (see Eq. (A.9)), while the corresponding vector (V) $\beta\beta_{0\nu}$ matrix element $M_V^{0\nu}$ is substantially reduced, and the full matrix element $M^{0\nu}$, which mainly comes from the axial-vector (A) moment $M_A^{0\nu}$, is reduced by $\approx 10\%$. The parameter $g_{pp}^{T=0}$ is fitted in the usual way with the requirement that the calculated values of the full $\beta\beta_{2\nu}$ matrix elements $M^{2\nu}$ agree with their experimental values. On the other hand, the PSU4SR has been also studied recently in the framework of schematic models [12, 13].

To implement the PSU4SR, we use a recipe based on energetics of F and GT resonances (in the particle-hole (ph) channel), and on the minima of F and GT β^+-strengths (in the particle-particle (pp) channel). Thus, the physical substratum is the same as in our previous QRPA work on the same issue [14–23, 25–28], and here we just bring up to date those studies. To implement this, we have to take into account the pseudoscalar (P) and weak-magnetism (M) matrix elements $M_P^{0\nu}$, and $M_M^{0\nu}$, as suggested by Šimkovic *et al.* [29] (see also[30, Appendix A]), which we have not done before, *i.e.,* we consider now the full nuclear weak current

$$\begin{aligned} J^{\mu\dagger}(\mathbf{x}) &= \bar{\Psi}(\mathbf{x})\tau^+ \left[g_V\gamma^\mu - g_A\gamma^\mu\gamma_5 \right. \\ &- \left. ig_M \frac{\sigma^{\mu\nu}q_\nu}{2M_N} - g_P q^\mu\gamma_5 \right] \Psi(\mathbf{x}), \end{aligned} \tag{1.1}$$

and not only the usual V and A terms, which we have discussed so far. We use the standard notation [25, 27, 29, 30].

The main features of our formalism are:

1. We solve the RPA equations only once for the intermediate $(N-1, Z+1)$ nucleus [23–27], while it is usually solved twice for (N, Z) and $(N-2, Z+2)$ nuclei, followed by some kind of averaging procedure. This is an outstanding difference since, as shown bellow, the one-QRPA method yields significantly smaller $\beta\beta_{0\nu}$ moments than the currently used two-QRPA-method.

2. The residual interaction is described by the δ-force (in units of MeV·fm^3)

$$V = -4\pi(v^s P_s + v^t P_t)\delta(r), \tag{1.2}$$

where the spin-singlet and spin-triplet parameters in the pp channel, *i.e.,* v_{pp}^s and v_{pp}^t correspond, respectively, to $g_{pp}^{T=1}$ and $g_{pp}^{T=0}$.

3. In essence, v_{pp}^s is fixed in the same way as $g_{pp}^{T=1}$. Namely, we require that the vector β^+-strength S_F^+ (defined in (2.31)) becomes minimal, which is achieved when the ratio $s = v_{pp}^s/\overline{v}_{pair}^s$ becomes $s_{sym} = 1$, with $\overline{v}_{pair}^s = (v_{pair}^s(\mathrm{p}) + v_{pair}^s(\mathrm{n}))/2$. This is a strong sign that the isospin symmetry is restored within the QRPA, leading to

$$S_F^+ \cong 0, M_F^{2\nu} \cong 0, M_V^{0\nu}(J^\pi = 0^+) \cong 0, \tag{1.3}$$

as well as to the concentration of the vector β^- strength S_F^- in the Isobaric Analog State (IAS); see Fig. 1 in Ref. [21]; $M_V^{0\nu}(J^\pi = 0^+)$ stands for the contribution of the intermediate states $J^\pi = 0^+$ to the NM $M_V^{0\nu}$.

4. To fix the parameter v_{pp}^t, we follow the same recipe as in the case of v_{pp}^s, *i.e.,* we require that the GT β^+ strength S_{GT}^+ (defined in (2.32)) becomes minimal, which indicates the PSU4SR, as was shown in Figs. 2 and 3 in Ref. [21], and Figs. 4.5 and 4.6 in Ref. [28]. For the corresponding pp ratio $t = v_{pp}^t/\overline{v}_{pair}^s$, we obtain now $t_{sym} \neq 1$, with

$$S_{GT}^+ \neq 0, M_{GT}^{2\nu} \neq 0, M_A^{0\nu}(J^\pi = 1^+) \neq 0, \tag{1.4}$$

and not all GT β^- strength S_{GT}^- is concentrated in the GT resonance (GTR); $M_A^{0\nu}(J^\pi = 1^+)$ has similar meaning to $M_V^{0\nu}(J^\pi = 0^+)$ in (1.3).

5. The important difference with other studies is that the experimental $\beta\beta_{2\nu}$ moments are not used for gauging the isoscalar pp parameter t. In this way, the QRPA model turns out to be predictive regarding $M^{2\nu}$. As a matter of fact, in Ref. [9], and in most of the QRPA calculations, the condition imposed on $g_{pp}^{T=0}$ is to reproduce the value of $\left|\mathcal{M}_{exp}^{2\nu}\right|$, with the justification that $\mathcal{M}^{0\nu}$ and $\mathcal{M}^{2\nu}$ are similar. It is true that they have in common the fact of connecting the same nuclear states, and transforming two neutrons into two protons, but dynamically they are quite different: while in the $\beta\beta_{2\nu}$-decay

renormalization effect for the GT moments and for the spin-magnetic moments may be viewed as a trend away from the (jj) coupling scheme toward the LS coupling." Equivalently, it can be stated that the residual interaction "restores" the $SU(4)$ symmetry. See also Refs. [6, 7].

two on-shell Dirac neutrinos are emitted, in the $\beta\beta_{0\nu}$-decay an off-shell Majorana neutrino is exchanged. As a consequence, in the first case the momentum transfer is of the order of a few MeV, which makes the long wavelength approximation valid, and only the allowed (F and GT) operators need to be considered. Instead, in the second case, the momentum transfer is $\sim 100 - 200$ MeV and many V and A multipoles contribute; more still, the induced P and M currents, whose effects are very small in the $\beta\beta_{2\nu}$-decay [27], also contribute quite significantly.

6. The restoration of the isospin and $SU(4)$ symmetries, broken in the mean field approximations, are manifested not only in the pp channel but also in the particle-hole ph channel. In fact, we have monitored the ph parameters v_s^{ph} and v_t^{ph} from the experimental energetics of the IAS and the GTR (in units of MeV) [31]:

$$E_{GTR} - E_{IAS} = 26A^{-1/3} - 18.5(N-Z)/A, \qquad (1.5)$$

where the first term on the rhs comes from the $SU(4)$ symmetry-breaking caused by the spin-orbital coupling, while the second term may be interpreted as the symmetry-restoration effect induced by the residual interaction [31–33], which displaces the GT towards the IAS with increasing $N - Z$ [31–33].

In short, we can say that in our nuclear model there are no free parameters.

This article is organized as follows: in Sec. II we elaborate a formalism, based on the Fourier-Bessel expansion introduced previously [21, 22, 25–27], which allows us to evaluate in a rather simple way the pseudoscalar and weak magnetism operators, such as they appear in weak current (1.1). In Sec. III we discuss the different QRPA methods that are employed in the evaluation of the $\beta\beta$-decay NM, pointing out the advantages of using just one QRPA equation instead of two, as is often done. In Sec. IV A we explain the determination of the model parameters, both in particle-hole (ph) and particle-particle (pp) channels, which restore the $SU(4)$ symmetry and are used in the evaluation of the $\beta\beta$-decay moments. In this section, extensive numerical evaluations of the NM are presented as well, by solving only one QRPA equation. Those for the 2ν-decays are confronted with the experimental data, while the predicted 0ν values are compared with some recent calculations. In Sec IV B we perform the calculations of the 0ν NM in the standard way, *i.e.,* by solving two QRPA equations, and by adjusting the isoscalar strength to the measured $\beta\beta_{2\nu}$ half-life. This allows us to directly compare our results with the recent QRPA calculations performed with realistic nucleon-nucleon (NN) forces, and thus discern and clarify the size of the following effects: a) two QRPA diagonalizations, b) the chosen type of NN interaction, and c) of how to set the parameters of the nuclear Hamiltonian. Different calculations of the $\beta\beta_{0\nu}$ NM are confronted in Sec. V and a few final remarks are made. Finally, in the Appendix the QRPA quenching mechanism in the Single-Mode Model (SMM), which is the simplest version of the $\beta\beta$-QRPA with only one intermediate state for each J^π [16, 22], is discussed.

II. FORMALISM

A. $\beta\beta_{0\nu}$ Nuclear Moments

The $\beta\beta_{0\nu}$ nuclear moments for the decay from the ground state $|I\rangle$ in the (N, Z) nucleus to the ground state $|F\rangle$ in the $(N-2, Z+2)$ nucleus (with energies E_I and E_F and spin and parity $J^\pi = 0^+$) can be expressed as (see, for instance, Eq. (14) in Ref. [25])

$$M^{0\nu} = \frac{\mathsf{R}}{4\pi} \sum_N \int d\mathbf{k} v(k;N) \mathsf{M}^{0\nu}(\mathbf{k};N) \qquad (2.1)$$

with

$$\begin{aligned} \mathsf{M}^{0\nu}(\mathbf{k};N) &\equiv \langle F|J_\mu^\dagger(-\mathbf{k})|N\rangle \\ &\times \langle N|J^{\mu\dagger}(\mathbf{k})|I\rangle \end{aligned} \qquad (2.2)$$

and

$$J^{\mu\dagger}(\mathbf{k}) = \int d\mathbf{x} J^{\mu\dagger}(\mathbf{x}) e^{-i\mathbf{k}\cdot\mathbf{x}}, \qquad (2.3)$$

is the Fourier transform of the hadronic current (1.1) in momentum space. Moreover, $\mathsf{R} = r_0 A^{1/3}$, with $r_0 = 1.2$ fm is introduced to make the 0ν NM dimensionless, and

$$v(k;N) = \frac{2}{\pi} \frac{1}{k(k+\omega_N)}, \qquad (2.4)$$

with

$$\omega_N = E_N - \frac{1}{2}(E_I + E_F). \qquad (2.5)$$

as the neutrino potential, where $k = |\mathbf{k}|$ is the modulus of the spatial part of the four transfer momentum, and the summation goes over all intermediate states N.

Within the impulse Non-Relativistic Approximation (NRA), and when the velocity terms are omitted, the hadronic currents read [5, 25–27, 34],

$$J^\mu_{NRA}(\mathbf{x}) = \Big(\rho(\mathbf{x}), \mathbf{j}(\mathbf{x})\Big) \qquad (2.6)$$

where

$$\begin{aligned} \rho(\mathbf{x}) &= g_V \sum_n \tau_n^+ \delta(\mathbf{x} - \mathbf{r}_n), \\ \mathbf{j}(\mathbf{x}) &= \sum_n \tau_n^+ \delta(\mathbf{x} - \mathbf{r}_n) [-g_A \boldsymbol{\sigma}_n \\ &+ f'_M \boldsymbol{\nabla} \times \boldsymbol{\sigma}_n - g'_P \boldsymbol{\nabla} \boldsymbol{\nabla} \cdot \boldsymbol{\sigma}_n], \end{aligned} \qquad (2.7)$$

are the one-body densities and currents, with $f_M = g_V + g_M$, and $f'_M = f_M/(2M_N), g'_P = g_P/(2M_N)$.

The intermediate-energy-dependent moments (2.2) are expressed in the form:

$$\mathsf{M}^{0\nu}(\mathbf{k};N) = \sum_X \mathsf{M}^{0\nu}_X(\mathbf{k};N), \tag{2.8}$$

with $X = V, A, P, M$, and [2]

$$\begin{aligned}
\mathsf{M}^{0\nu}_V(\mathbf{k};N) &= g_V^2\langle F|\sum_n \tau_n^+ e^{i\mathbf{k}\cdot\mathbf{r}_n}|N\rangle \\
&\quad \langle N|\sum_m \tau_m^+ e^{-i\mathbf{k}\cdot\mathbf{r}_m}|I\rangle, \\
\mathsf{M}^{0\nu}_A(\mathbf{k};N) &= -g_A^2\langle F|\sum_n \tau_n^+ \boldsymbol{\sigma}_n e^{i\mathbf{k}\cdot\mathbf{r}_n}|N\rangle \\
&\quad \cdot\ \langle N|\sum_m \tau_m^+ \boldsymbol{\sigma}_m e^{-i\mathbf{k}\cdot\mathbf{r}_m}|I\rangle, \\
\mathsf{M}^{0\nu}_P(\mathbf{k};N) &= -g'_P(g'_P k^2 - 2g_A) \\
&\quad \langle F|\sum_n \tau_n^+ \boldsymbol{\sigma}_n\cdot\mathbf{k} e^{i\mathbf{k}\cdot\mathbf{r}_n}|N\rangle \\
&\quad \langle N|\sum_m \tau_m^+ \boldsymbol{\sigma}_m\cdot\mathbf{k} e^{-i\mathbf{k}\cdot\mathbf{r}_m}|I\rangle, \\
\mathsf{M}^{0\nu}_M(\mathbf{k};N) &= f'^2_M\langle F|\sum_n \tau_n^+ \boldsymbol{\sigma}_n\times\mathbf{k} e^{i\mathbf{k}\cdot\mathbf{r}_n}|N\rangle \\
&\quad \cdot\ \langle N|\sum_m \tau_m^+ \boldsymbol{\sigma}_m\times\mathbf{k} e^{-i\mathbf{k}\cdot\mathbf{r}_m}|I\rangle.
\end{aligned} \tag{2.9}$$

The multipole expansion of NM is performed here, using the Fourier-Bessel relationship

$$e^{i\mathbf{k}\cdot\mathbf{r}} = 4\pi\sum_L i^L j_L(kr)(Y_L(\hat{\mathbf{k}})\cdot Y_L(\hat{\mathbf{r}})), \tag{2.10}$$

to express them in terms of spherical tensor operators

$$\begin{aligned}
\mathsf{Y}_{JM}(k) &= \sum_n \tau_n^+ j_J(kr_n) Y_{JM}(\hat{\mathbf{r}}_n), \\
\mathsf{S}_{LJM}(k) &= \sum_n \tau_n^+ j_L(kr_n)[\boldsymbol{\sigma}_n\otimes Y_L(\hat{\mathbf{r}}_n)]_{JM}.
\end{aligned} \tag{2.11}$$

In this way, and after performing the angular integration on Ω_k,

$$\int d\Omega_k \mathsf{M}^{0\nu}_X(\mathbf{k},N) \equiv \mathsf{M}^{0\nu}_X(k,N), \tag{2.12}$$

one obtains

$$\begin{aligned}
\mathsf{M}^{0\nu}_V(k,N) &= g_V^2(4\pi)^2\sum_J \langle F|\mathsf{Y}_J(k)|N\rangle\langle N|\mathsf{Y}_J(k)|I\rangle, \\
\mathsf{M}^{0\nu}_A(k,N) &= g_A^2(4\pi)^2\sum_{LJ}(-1)^{L+J}\langle F|\mathsf{S}_{LJ}(k)|N\rangle \\
&\quad \cdot\ \langle N|\mathsf{S}_{LJ}(k)|I\rangle, \\
\mathsf{M}^{0\nu}_P(k,N) &= g'_P(g'_P k^2 - 2g_A)(4\pi)^2\sum_{LL'Jl}(-)^{(L+L')/2} \\
&\quad \times\ (11|l)(LL'|l)\hat{L}\hat{L}'\begin{Bmatrix} 1 & 1 & l \\ L & L' & J\end{Bmatrix} \\
&\quad \times\ \langle F|\mathsf{S}_{LJ}(k)|N\rangle\cdot\langle N|\mathsf{S}_{L'J}(k)|I\rangle \\
\mathsf{M}^{0\nu}_M(k,N) &= -f'^2_M(k^2)(4\pi)^2\sum_{LL'Jl}(-)^{(L+L')/2}\hat{L}\hat{L}' \\
&\quad \times\ (11|l)(LL'|l)\begin{Bmatrix} 1 & 1 & l \\ L & L' & J\end{Bmatrix}[2-l(l+1)/2] \\
&\quad \times\ \langle F|\mathsf{S}_{LJ}(k)|N\rangle\cdot\langle N|\mathsf{S}_{L'J}(k)|I\rangle.
\end{aligned} \tag{2.13}$$

The expression (2.1) is written again in the form (2.8), *i.e.,* as $M^{0\nu} = \sum_X M^{0\nu}_X$, where the moments $M^{0\nu}_X$ are derived from the moments (2.13) after multiplying them by the factor $\mathsf{R}k^2 v(k;N)/4\pi$, and integrating over k. For instance,

$$\begin{aligned}
M^{0\nu}_A &= 4\pi\mathsf{R}g_A^2\sum_{LJN}(-1)^{L+J}\int v(k,N)k^2dk \\
&\quad \times\ \langle F|\mathsf{S}_{LJ}(k)|N\rangle\cdot\langle N|\mathsf{S}_{LJ}(k)|I\rangle.
\end{aligned} \tag{2.14}$$

To incorporate the nuclear structure, we employ the relation (see [25, Eq. 36)])

$$\begin{aligned}
&\sum_N \langle F|\mathsf{T}_J(k)|N\rangle\cdot\langle N|\mathsf{T}_J(k)|I\rangle \\
&= (-)^J\sum_{\alpha\pi pnp'n'}\rho^{ph}(pnp'n';J^\pi_\alpha) \\
&\quad \times\ \langle p||\mathsf{T}_J(k)||n\rangle\langle p'||\mathsf{T}_J(k)||n'\rangle,
\end{aligned} \tag{2.15}$$

where

$$\rho^{ph}(pnp'n';J^\pi_\alpha) = \rho^-(pn;J^\pi_\alpha)\rho^+(p'n';J^\pi_\alpha), \tag{2.16}$$

and

$$\begin{aligned}
\rho^-(pnJ^\pi_\alpha) &= \hat{J}^{-1}\langle 0^+_F||(a^\dagger_p a_{\bar{n}})_{J^\pi}||J^\pi_\alpha\rangle \\
\rho^+(pnJ^\pi_\alpha) &= \hat{J}^{-1}\langle J^\pi_\alpha||(a^\dagger_p a_{\bar{n}})_{J^\pi}||0^+_I\rangle,
\end{aligned} \tag{2.17}$$

are the $\beta^\mp$ one-body state dependent ph density matrices, the index α labels different intermediate states with the same spin J and parity π, and $\hat{J}\equiv\sqrt{2J+1}$. For convenience, we made the substitution

$$|I\rangle, |F\rangle, |N\rangle \rightarrow |0^+_I\rangle, |0^+_F\rangle, |J^\pi_\alpha\rangle. \tag{2.18}$$

For example, Eq. (2.14) reads now

$$\begin{aligned}
M^{0\nu}_A &= 4\pi\mathsf{R}g_A^2\sum_{LJ}(-1)^{1+L}\sum_{\alpha\pi pnp'n'}\rho^{ph}(pnp'n';J^\pi_\alpha) \\
&\quad \times\ \int v(k,\omega_{J^\pi_\alpha})k^2dk\langle p||\mathsf{S}_{LJ}(k)||n\rangle\langle p'||\mathsf{S}_{LJ}(k)||n'\rangle.
\end{aligned} \tag{2.19}$$

[2] For the sake of convenience, the standard F and GT $\beta\beta_{0\nu}$ moments will be labeled, respectively, as V and A moments.

Thus, the final results for the $\beta\beta_{0\nu}$ NM are:

$$\begin{aligned}
M^{0\nu}_V &= \sum_{J^\pi_\alpha}(-)^J \sum_{pp'nn'} \rho^{ph}(pnp'n';J^\pi_\alpha) \\
&\times W_{J0J}(pn)W_{J0J}(p'n')\mathcal{R}^V_{JJ}(pnp'n';\omega_{J^\pi_\alpha}), \\
M^{0\nu}_A &= \sum_{LJ^\pi_\alpha}(-)^{L+1} \sum_{pp'nn'} \rho^{ph}(pnp'n';J^\pi_\alpha) \\
&\times W_{L1J}(pn)W_{L1J}(p'n')\mathcal{R}^A_{LL}(pnp'n';\omega_{J^\pi_\alpha}), \\
M^{0\nu}_P &= -\sum_{J^\pi_\alpha LL'l}(-)^{J+(L+L')/2}\hat{L}\hat{L}'(LL'|l)(11|l) \\
&\times \sum_{pp'nn'} \rho^{ph}(pnp'n';J^\pi_\alpha)W_{L1J}(pn)W_{L'1J}(p'n') \\
&\times \left\{\begin{array}{ccc} L & L' & l \\ 1 & 1 & J \end{array}\right\}\mathcal{R}^P_{LL'}(pnp'n';\omega_{J^\pi_\alpha}), \\
M^{0\nu}_M &= -\sum_{J^\pi_\alpha LL'l}(-)^{J+(L+L')/2}\hat{L}\hat{L}'(LL'|l)(11|l) \\
&\times \sum_{pp'nn'} \rho^{ph}(pnp'n';J^\pi_\alpha)W_{L1J}(pn)W_{L'1J}(p'n') \\
&\times \left\{\begin{array}{ccc} L & L' & l \\ 1 & 1 & J \end{array}\right\}[2-l(l+1)/2]\mathcal{R}^M_{LL'}(pnp'n';\omega_{J^\pi_\alpha}),
\end{aligned} \tag{2.20}$$

with the angular parts: [3]

$$W_{LSJ}(pn) = \sqrt{2}\hat{S}\hat{J}\hat{L}\hat{l}_n\hat{j}_n\hat{j}_p(l_nL|l_p)\left\{\begin{array}{ccc} l_p & \frac{1}{2} & j_p \\ L & S & J \\ l_n & \frac{1}{2} & j_n \end{array}\right\}, \tag{2.21}$$

while the two-body radial integrals are defined as

$$\begin{aligned}
\mathcal{R}^X_{LL'}(pnp'n';\omega_{J^\pi_\alpha}) &= \mathsf{R}\int dkk^2 v_X(k;\omega_{J^\pi_\alpha}) \\
&\times R_L(pn;k)R_{L'}(p'n';k),
\end{aligned} \tag{2.22}$$

with

$$R_L(pn;k) = \int_0^\infty u_{n_pl_p}(r)u_{n_nl_n}(r)j_L(kr)r^2dr, \tag{2.23}$$

being one-body radial integrals, and u_{nl} the radial single-particle functions. Finally, the effective neutrino potentials in $v_X(k;\omega_{J^\pi_\alpha})$ (2.22) become

$$\begin{aligned}
v_V(k;\omega_{J^\pi_\alpha}) &= g^2_V(k^2)v(k;\omega_{J^\pi_\alpha}), \\
v_A(k;\omega_{J^\pi_\alpha}) &= g^2_A(k^2)v(k;\omega_{J^\pi_\alpha}), \\
v_M(k;\omega_{J^\pi_\alpha}) &= k^2 f'^2_M(k^2)v(k;\omega_{J^\pi_\alpha}), \\
v_P(k;\omega_{J^\pi_\alpha}) &= k^2 g'_P(k^2)[2g_A(k^2)-k^2g'_P(k^2)]v(k;\omega_{J^\pi_\alpha}),
\end{aligned} \tag{2.24}$$

[3] We use here the angular momentum coupling scheme $|(\frac{1}{2},l)j\rangle$.

where, within the new notation put forward in (2.18), Eqs. (2.4) and (2.5) are now expressed as

$$v(k;\omega_{J^\pi_\alpha}) = \frac{2}{\pi}\frac{1}{k(k+\omega_{J^\pi_\alpha})}, \tag{2.25}$$

with

$$\begin{aligned}
\omega_{J^\pi_\alpha} &= E_{J^+_\alpha} - \frac{E_{0_{+I}} + E_{0^+_F}}{2} \\
&= E_{J^+_\alpha} - E_{0^+_I} + \frac{1}{2}Q_{\beta\beta}
\end{aligned} \tag{2.26}$$

where $Q_{\beta\beta} = E_{0^+_I} - E_{0^+_F}$ is the Q-value of the $\beta\beta$-decay.

Finite Nucleon Size (FNS) effects are introduced through the usual dipole form factors

$$\begin{aligned}
g_V &\rightarrow g_V(k^2) \equiv g_V\left(\frac{\Lambda^2_V}{\Lambda^2_V+k^2}\right)^2, \\
g_A &\rightarrow g_A(k^2) \equiv g_A\left(\frac{\Lambda^2_A}{\Lambda^2_A+k^2}\right)^2, \\
f'_M &\rightarrow f'_M(k^2) \equiv f'_M\left(\frac{\Lambda^2_V}{\Lambda^2_V+k^2}\right)^2, \\
g'_P &\rightarrow g'_P(k^2) \equiv g'_P\left(\frac{\Lambda^2_A}{\Lambda^2_A+k^2}\right)^2,
\end{aligned} \tag{2.27}$$

as in Refs. [18, 29, 35], and $\Lambda_V = 0.85$ GeV and $\Lambda_A = 1.086$ GeV are the vectorial and axial-vectorial cut-off parameters, respectively.

The weak coupling constants in (1.1) are fixed as follows: $g_V = 1$ and $g_M = 3.7$ from Conservation of Vector Current (CVC), $g_A = 1.27$ from the experimental data [36], and $g_P = 2M_N g_A/(q^2+m^2_\pi)$ from the assumption of Partially Conserved Axial Current (PCAC) [34].

The Short Range Correlations (SRC) between the two nucleons are taken into account in the standard way via the correlation function [37, 38]

$$f^{SRC}(r) = 1 - j_0(k_c r), \tag{2.28}$$

where $k_c = 3.93$ fm^{-1} is the Compton wavelength of the ω-meson. This leads to the following modification of the potentials $v_X(k;\omega_{J^\pi_\alpha})$ in the momentum space (see Eqs. (2.14) and (2.15) in Ref. [18], as well as Refs. [21, 25–28, 39].)

$$v_X(q;\omega_J) \rightarrow v_X(q;\omega_J) - \Delta v_X(q;\omega_J), \tag{2.29}$$

with

$$\begin{aligned}
\Delta v_X(q;\omega_J) &= \frac{1}{2q^2_c}\int_{-1}^1 dx \int dkk^2 v_X(k;\omega_J) \\
&\times \delta(\sqrt{q^2+k^2+2xqk}-q_c).
\end{aligned} \tag{2.30}$$

It is not difficult to show that

$$\begin{aligned}
\Delta v_X(q;\omega_J) &= \frac{1}{2}\int_{-1}^1 dx \\
&\times v_X(\sqrt{q^2+q^2_c+2xqq_c};\omega_J),
\end{aligned} \tag{2.31}$$

and this is the expression used to evaluate the SRC.

B. $\beta\beta_{2\nu}$ Matrix Element and Charge-Exchange Transition Strengths

Independently of the nuclear model used and only considering the allowed transitions, the $\beta\beta_{2\nu}$ moment reads

$$M^{2\nu} = M^{2\nu}_F + M^{2\nu}_{GT}, \tag{2.32}$$

with [21]

$$\begin{aligned} M^{2\nu}_F &= g_V^2 \sum_{pnp'n'\alpha} \rho^{ph}(pnp'n';0^\pi_\alpha) \frac{W_{000}(pn)W_{000}(p'n')}{\omega_{0^+_\alpha}}, \\ M^{2\nu}_{GT} &= -g_A^2 \sum_{pnp'n'\alpha} \rho^{ph}(pnp'n';1^\pi_\alpha) \frac{W_{011}(pn)W_{011}(p'n')}{\omega_{1^+_\alpha}}. \end{aligned} \tag{2.33}$$

The single charge-exchange $\beta^\mp$ strengths are also discussed here. They are

$$S^\mp_F = \sum_{pn\alpha} |\rho^\mp(pn0^+_\alpha) W_{000}(pn)|^2, \tag{2.34}$$

and

$$S^\mp_{GT} = \sum_{pn\alpha} |\rho^\mp(pn1^+_\alpha) W_{011}(pn)|^2. \tag{2.35}$$

III. CHARGE-EXCHANGE QRPA

All of the formalism presented in the previous section is valid in general, and any nuclear model can be used to evaluate the one-body density matrices (2.17). The most frequently used model is charge-exchange QRPA. It was formulated, and applied to allowed $\beta^\pm$-decays and collective GT resonance, by Halbleib and Sorensen (HS) in 1967 [40], as follows:

1) BCS equations for the initial even-even nucleus (N, Z) are solved to obtain the occupation coefficients (v_n, v_p), $(u_n = \sqrt{1-v_n^2}, u_p = \sqrt{1-v_p^2})$, the quasiparticle energies (ϵ_n, ϵ_p) and the chemical potentials (λ_n, λ_p) for neutrons and protons, as well as the ground state energy E_{0_i}, and the BCS vacuum

$$|0_I\rangle = \prod_p (u_p + v_p c^\dagger_p c^\dagger_{\bar{p}}) \prod_n (u_n + v_n c^\dagger_n c^\dagger_{\bar{n}})|\rangle, \tag{3.1}$$

where $|\rangle$ stands for the particle vacuum. The u's and v's in the parent nucleus are determined under the constraints

$$\sum_{j_p} (2j_p+1) v_p^2 = Z, \qquad \sum_n (2j_n+1) v_n^2 = N, \tag{3.2}$$

where Z and N are the number of protons and neutrons, respectively, in the parent nucleus.

2) Transition $\beta^\mp$-densities

$$\begin{aligned} \rho^-(pnJ^\pi_\alpha) &= u_p v_n X_{J^\pi_\alpha}(pn) + u_n v_p Y_{J^\pi_\alpha}(pn), \\ \rho^+(pnJ^\pi_\alpha) &= u_n v_p X_{J^\pi_\alpha}(pn) + u_p v_n Y_{J^\pi_\alpha}(pn), \end{aligned} \tag{3.3}$$

and excitation energies

$$E^{N\pm1,Z\mp1}_{J^\pi_\alpha} = E_{0^+_I} + \Omega_{J^\pi_\alpha} \pm \lambda_n \mp \lambda_p, \tag{3.4}$$

in neighboring odd-odd, $(N \pm 1, Z \mp 1)$, nuclei (see, for instance, [41, Sec. 6.3.4]), are obtained by solving the pn-QRPA equation

$$\begin{pmatrix} A_{J^\pi} & B_{J^\pi} \\ B_{J^\pi} & A_{J^\pi} \end{pmatrix} \begin{pmatrix} X_{J^\pi_\alpha} \\ Y_{J^\pi_\alpha} \end{pmatrix} = \Omega_{J^\pi_\alpha} \begin{pmatrix} X_{J^\pi_\alpha} \\ -Y_{J^\pi_\alpha} \end{pmatrix}, \tag{3.5}$$

for forward and backward going amplitudes, $X_{J^\pi_\alpha}(pn)$ and $Y_{J^\pi_\alpha}(pn)$, and QRPA excitation energies $\Omega_{J^\pi_\alpha}$ on vacuum (3.1). Both F and GT strengths, given by (2.34) and (2.35), fulfill the well known Ikeda sum rule

$$S^\beta = S^- - S^+ = N - Z. \tag{3.6}$$

It is important to mention that the ground state correlations (GSC) for the charge-changes decay $(N, Z) \xrightarrow{\beta^-} (N-1, Z+1)$ is the decay $(N, Z) \xrightarrow{\beta^+} (N+1, Z-1)$, and viceversa. In effect, the exchange $\rho^-(pnJ^\pi_\alpha) \leftrightarrow \rho^+(pnJ^\pi_\alpha)$ in (3.3) is obtained from the exchange $X_{J^\pi_\alpha}(pn) \leftrightarrow Y_{J^\pi_\alpha}(pn)$.

When the QRPA is applied to $\beta\beta$-decay, one has to deal simultaneously with two ground states E_{0_I} and E_{0_F}, which requires further steps in modeling the theory in order to end up with some sort of averaging. This is inevitable, even in the case of particle number projected QRPA [19].

A. Method I

Intensive implementations of QRPA to $\beta\beta$-decay began only about 20 years after the HS work [40], when Vogel and Zirnbauer [42] discovered that the GSC play an essential role in suppressing the $\beta\beta_{2\nu}$ rates. Their QRPA calculations of $M^{2\nu}_{GT}$ are carried out for both the initial and final nuclei and the resulting matrix elements are averaged. That is, they repeat the steps 1) and 2) for the (N, Z) and $(N-2, Z+2)$ ground states, and for intermediate states 1^+_α and $\bar{1}^+_\alpha$ in the nucleus $(N-1, Z+1)$. In the second case the BCS vacuum is

$$|0_F\rangle = \prod_p (\bar{u}_p + \bar{v}_p c^\dagger_p c^\dagger_{\bar{p}}) \prod_n (\bar{u}_n + \bar{v}_n c^\dagger_n c^\dagger_{\bar{n}})|\rangle, \tag{3.7}$$

derived under the constraints

$$\sum_p (2j_p+1) \bar{v}_p^2 = Z+2, \quad \sum_n (2j_n+1) \bar{v}_n^2 = N-2, \tag{3.8}$$

which fulfill the sum rule

$$\bar{S}^{\beta} = N - Z - 4. \tag{3.9}$$

The energy denominator $\omega_{1^+_\alpha}$ in (2.33) can be evaluated from experimental data or self-consistently within the BCS-QRPA framework. When the latter is performed, one finds that [41, Sec. 6.3.4]

$$Q_{\beta\beta} = E_{0^+_I} - E_{0^+_F} = 2(\lambda_n - \lambda_p), \tag{3.10}$$

and, therefore, from (3.5)

$$E_{1^+_\alpha} - E_{0^+_I} = \Omega_{1^+_\alpha} - \frac{1}{2}Q_{\beta\beta}, \tag{3.11}$$

which from (2.26) yields

$$\omega_{1^+_\alpha} \;=\; \Omega_{1^+_\alpha}. \tag{3.12}$$

Proceeding in the same way for the final state 0_F, one finds that the averaged GT moment is:

$$\begin{aligned} M^{2\nu}_{GT} \;&=\; -\frac{g_A^2}{2}\sum_{pnp'n'\alpha} W_{011}(pn)W_{011}(p'n') \\ &\times\; \left[\frac{\rho^{ph}(pnp'n';1^+_\alpha)}{\Omega_{1^+_\alpha}} + \frac{\rho^{ph}(pnp'n';\bar{1}^+_\alpha)}{\Omega_{\bar{1}^+_\alpha}}\right]. \end{aligned} \tag{3.13}$$

B. Method II

Shortly after the discovery of the importance of the GSC in Ref. [42], Civitarese, Faessler and Tomoda [43] made their calculations, repeating the steps 1) and 2) for the ground states of (N, Z) and $(N-2, Z+2)$ nuclei, and for intermediate states 1^+_α and $1^+_{\alpha'}$ in the $(N-1, Z+1)$ nucleus, and arrived at the same conclusion about the importance of the GSC (see also Ref. [44]). In our notation, their $\beta\beta_{2\nu}$ moment reads

$$\begin{aligned} M^{2\nu}_{GT} \;&=\; -g_A^2\sum_{pnp'n'\alpha\alpha'} W_{011}(pn)W_{011}(p'n') \\ &\times\; \frac{\rho^{ph}(pn;1^+_\alpha)\langle 1^+_\alpha|\bar{1}^+_{\alpha'}\rangle\rho^{ph}(p'n';\bar{1}^+_{\alpha'})}{m_e c^2 + \frac{1}{2}Q_{\beta\beta} + E_{1^+_\alpha} - E_{0_i}}, \end{aligned} \tag{3.14}$$

where the overlap is given by

$$\langle 1^+_\alpha|\bar{1}^+_{\alpha'}\rangle \;=\; \sum_{pn}\left[X_{1^+_\alpha}(pn)X_{\bar{1}^+_{\alpha'}}(pn) - Y_{1^+_\alpha}(pn)Y_{\bar{1}^+_{\alpha'}}(pn)\right]. \tag{3.15}$$

This overlap is introduced since the intermediate states $|1^+_\alpha\rangle$ and $|\bar{1}^+_{\alpha'}\rangle$, being generated from different ground states, are not orthogonal to each other. When this non-orthogonality is very pronounced the numerical results could be eventually unreliable. Making use of (3.11) the energy denominators in (3.14) become $m_e c^2 + \Omega_{1^+_\alpha}$.
In more recent applications of Method II [45, 46, 72] this denominator was replaced by $(\Omega_{1^+_\alpha} + \Omega_{\bar{1}^+_{\alpha'}})/2$. Moreover, the BCS overlap factor $\langle 0^+_I|0^+_F\rangle$, which is about 0.8, has been incorporated in these last studies. Thus, the $\beta\beta_{2\nu}$ moment reads

$$\begin{aligned} M^{2\nu}_{GT} \;&=\; -2g_A^2\langle 0^+_I|0^+_F\rangle\sum_{pnp'n'\alpha\alpha'} W_{011}(pn)W_{011}(p'n') \\ &\times\; \frac{\rho^{+}(p'n';\bar{1}^+_{\alpha'})\langle\bar{1}^+_{\alpha'}|1^+_\alpha\rangle\rho^{-}(pn;1^+_\alpha)}{\Omega_{1^+_\alpha} + \Omega_{\bar{1}^+_{\alpha'}}}, \end{aligned} \tag{3.16}$$

where

$$\langle 0^+_I|0^+_F\rangle = \prod_p(u_p\bar{u}_p + v_p\bar{v}_p)\prod_n(u_n\bar{u}_n + v_n\bar{v}_n). \tag{3.17}$$

The following substitutions have to be made in the evaluation of the $\beta\beta_{0\nu}$ moments:

$$\begin{aligned} \sum_{J^\pi_\alpha} \quad &\rho^{ph}(pnp'n';J^\pi_\alpha) \to \langle 0^+_I|0^+_F\rangle \times \\ &\sum_{J^\pi\alpha\alpha'}\rho^{+}(p'n';\bar{J}^+_{\alpha'})\langle\bar{J}^+_{\alpha'}|J^+_\alpha\rangle\rho^{-}(pn;J^+_\alpha), \end{aligned} \tag{3.18}$$

in (2.20), together with

$$\omega_{J^\pi_\alpha} \to (\Omega_{J^+_\alpha} + \Omega_{\bar{J}^+_{\alpha'}})/2, \tag{3.19}$$

in (2.25).

C. Method III

The above equations (3.13) and (3.14) for $M^{2\nu}_{GT}$ cannot be derived mathematically, but they are physically sound ansatz for the HS equations (3.1)-(3.6) originally designed for the single β-decay, to make possible the calculations of $\beta\beta$-decay. In view of this, a new pn-QRPA, specially tailored for the last processes, was derived analytically in Ref. [16]. It is based on appropriate canonical quasi-particle transformations for which the GSC for the $\beta^\mp$ transitions in the intermediate $(N-1, Z+1)$ nucleus are the $\beta^\pm$ transitions in the same nucleus. [4] Only one QRPA equation

$$\begin{pmatrix} \tilde{A}_{J^\pi} & \tilde{B}_{J^\pi} \\ \tilde{B}_{J^\pi} & \tilde{A}_{J^\pi} \end{pmatrix}\begin{pmatrix} \tilde{X}_{J^\pi_\alpha} \\ \tilde{Y}_{J^\pi_\alpha} \end{pmatrix} = \tilde{\Omega}_{J^\pi_\alpha}\begin{pmatrix} \tilde{X}_{J^\pi_\alpha} \\ -\tilde{Y}_{J^\pi_\alpha} \end{pmatrix}, \tag{3.20}$$

[4] The intermediate $(N-1, Z+1)$ nucleus is now represented as a combination of proton-particle neutron-hole excitations on the initial (N, Z) nucleus, and of proton-hole neutron-particle excitations on the final $(N-2, Z+2)$ nucleus.

is solved for the vacuum

$$|\tilde{0}\rangle = \prod_p (u_p + \bar{v}_p c_p^\dagger c_{\bar{p}}^\dagger) \prod_n (\bar{u}_n + v_n c_n^\dagger c_{\bar{n}}^\dagger)|\rangle, \qquad (3.21)$$

which contains information on both initial and final ground states. Unbarred and barred quantities are derived as before, *i.e.,* by solving the BCS equations for initial and final nuclei with constraints (3.2) and (3.8), respectively. The matrices $\tilde{A}_{J^\pi}$ and $\tilde{B}_{J^\pi}$ are given by [16, Eq. (3)], and the GT moment is:

$$\begin{aligned} M^{2\nu}_{GT} &= -g_A^2 \sum_{pnp'n'\alpha} W_{011}(pn) W_{011}(p'n') \\ &\times \frac{\tilde{\rho}^-(pn1^+_\alpha)\tilde{\rho}^+(p'n'1^+_\alpha)}{\tilde{\Omega}_{1^+_\alpha}} \end{aligned} \qquad (3.22)$$

where

$$\begin{aligned} \tilde{\rho}^-(pnJ^\pi_\alpha) &= \sqrt{\sigma_p\sigma_n}(u_p v_n \tilde{X}_{J^\pi_\alpha}(pn) + \bar{u}_n \bar{v}_p \tilde{Y}_{J^\pi_\alpha}(pn)), \\ \tilde{\rho}^+(pnJ^\pi_\alpha) &= \sqrt{\sigma_p\sigma_n}(\bar{v}_p \bar{u}_n \tilde{X}_{J^\pi_\alpha}(pn) + u_p v_n \tilde{Y}_{J^\pi_\alpha}(pn)), \end{aligned} \qquad (3.23)$$

and

$$\sigma_p^{-1} = u_p^2 + \bar{v}_p^2, \quad \sigma_n^{-1} = u_n^2 + \bar{v}_n^2. \qquad (3.24)$$

The GT strengths

$$\tilde{S}^\mp_{GT} = \sum_{pn\alpha} |\tilde{\rho}^\mp(pn1^+_\alpha) W_{011}(pn)|^2, \qquad (3.25)$$

fulfill now the sum rule

$$\tilde{S}^\beta = \tilde{S}^- - \tilde{S}^+ \cong N - Z - 2. \qquad (3.26)$$

Note that here the averaging is no longer carried out at the level of the QRPA but within the BCS approximations.

In addition to being mathematically and physically justified, Method III has several advantages over Methods I and II, namely: i) only one QRPA equation is solved instead of two, ii) it is not necessary to deal with troublesome overlaps (3.15), iii) $M^{2\nu}_{GT}$ can be evaluated without diagonalizing the QRPA matrix (3.16); it is enough to invert this matrix [16], and iv) it allows us to formulate the SMM, which illustrates several aspects of the PSU4SR and the role played by the GSC [18], as shown in the Appendix.

D. Method IV

In his studies of single β-decay, Cha [48] has argued that "because the intersection between two-qp's takes place in a residual nucleus, we should calculate ϵ's, u's, and v's in the daughter nucleus." Motivated by this argument, and in order to make the QRPA calculation as simple as possible without losing the physical content of the model, a further step was taken in Ref. [23] in the evaluation of the moments $M^{2\nu}_{GT}$. There, instead of dealing with the two-vacua QRPA, as done in Ref. [16], BCS equations are solved only for the intermediate nucleus, obtaining the vacuum

$$|0'_{int}\rangle = \prod_p (u'_p + v'_p c_p^\dagger c_{\bar{p}}^\dagger) \prod_n (u'_n + v'_n c_n^\dagger c_{\bar{n}}^\dagger)|\rangle, \qquad (3.27)$$

where the u''s and v''s are determined under the constraints

$$\sum_p (2j_p+1) v'^2_p = Z+1, \quad \sum_n (2j_n+1) v'^2_n = N-1, \qquad (3.28)$$

satisfying the sum rule

$$S'^{\beta^-} = N - Z - 2 \qquad (3.29)$$

for β^--decay, which is very similar to (3.26).

In a manner similar to (3.22), the GT moment is

$$\begin{aligned} M^{2\nu}_{GT} &= -g_A^2 \sum_{pnp'n'\alpha} W_{011}(pn) W_{011}(p'n') \\ &\times \frac{\rho'^-(pn1^+_\alpha)\rho'^+(p'n'1^+_\alpha)}{\Omega'_{1^+_\alpha}}, \end{aligned} \qquad (3.30)$$

where the primed quantities have the same meaning as the corresponding unprimed ones in (3.3) and (3.4). The $\beta\beta_{0\nu}$-moments are evaluated in the same way. That is, Eq. (2.16) is evaluated as

$$\rho^{ph}(pnp'n'; J^\pi_\alpha) = \rho'^-(pn; J^\pi_\alpha)\rho'^+(p'n'; J^\pi_\alpha), \qquad (3.31)$$

and Eq. (2.25) as

$$v(k; \omega_{J^\pi_\alpha}) = v(k; \Omega'_{J^\pi_\alpha}). \qquad (3.32)$$

Finally, the unperturbed (BCS) one body densities are

$$\begin{aligned} \rho'^-_{BCS}(pnJ^\pi_\alpha) &= u'_p v'_n, \\ \rho'^+_{BCS}(pnJ^\pi_\alpha) &= u'_n v'_p. \end{aligned} \qquad (3.33)$$

As already pointed out in Ref. [49], the two-QRPA Methods I and II involve also the nuclei $(N+1, Z-1)$ and $(N-3, Z+3)$. This is so because the GSC for the transitions $(N,Z) \xrightarrow{\beta^-} (N-1, Z+1)$ and $(N-1, Z+1) \xrightarrow{\beta^-} (N-2, Z+2) \cong (N-2, Z+2) \xrightarrow{\beta^+} (N-1, Z+1)$ correspond, respectively, to transitions $(N,Z) \xrightarrow{\beta^+} (N+1, Z-1)$ and $(N-2, Z+2) \xrightarrow{\beta^-} (N-3, Z+3)$. On the contrary, the one-QRPA Methods III and IV only involve the nuclei within the isobaric triplet (N,Z), $(N-1, Z+1)$, $(N-2, Z+2)$ where the $\beta\beta$-decay occurs. Also, in the last methods, similarly to what happens in the single β-decay, the GSC for the decay $(N,Z) \xrightarrow{\beta^-} (N-1, Z+1)$ is the decay $(N-1, Z+1) \xrightarrow{\beta^-} (N-2, Z+2) \cong (N-2, Z+2) \xrightarrow{\beta^+} (N-1, Z+1)$, and vice versa.

Shortly after having been formulated, all four methods were extended to the $\beta\beta_{0\nu}$ moments [21, 22, 24–26, 50,

51], where the importance of the GSC was evidenced once again. However, Method IV is being used here for the first time in a simultaneous study of both double decay beta modes. This was precisely the main motivation to present the numerical results that follow, based on this one-QRPA method, and by fixing the isoscalar strength t from the PSU4SR.

IV. NUMERICAL RESULTS

A. Method IV with t from PSU4SR

As explained in Sec. I, within our modus operandi all nuclear model parameters are fixed. To set them in the ph channel we use the energetics of the IAS and GTR [31], with the result $v^s_{ph} = 55$ and $v^t_{ph} = 92$ in units of MeV$\cdot$ fm^3. These values are used for all nuclei, with exception of ^{48}Ca where $v^s_{ph} = 27$ and $v^t_{ph} = 64$ were employed. Within the pp channel, v^s_{pp} and v^t_{pp}, or more precisely, the ratios s and t, are determined from the condition that the strengths S^+_F and S^+_{GT} become minimal.

TABLE I: Values of the parameters s_{sym} and t_{sym}, and experimental and calculated energies of the IAS and GTR in the initial nucleus. The energies are given in units of MeV.

^AZ	s_{sym}	t_{sym}	E^{cal}_{IAS}	E^{exp}_{IAS}	E^{cal}_{GTR}	E^{exp}_{GTR}
^{48}Ca	1.00	1.20	8.70	7.36	13.66	11.43
^{76}Ge	1.00	1.23	11.47	10.21	13.92	13.42
^{82}Se	1.00	1.30	12.25	10.59	15.59	13.41
^{96}Zr	1.00	1.55	14.18	11.85	16.10	14.45
^{100}Mo	1.00	1.49	13.70	12.29	15.83	14.93
^{128}Te	1.00	1.41	13.74	14.06	14.36	15.75
^{130}Te	1.00	1.45	14.71	13.98	14.95	15.42
^{150}Nd	1.00	1.29	20.21	15.42	18.46	16.61

Fig. 1 shows the behavior of vector observables as a function of s (on the left side), and axial-vector observable as a function of t (on the right side) for ^{48}Ca, ^{76}Ge, ^{82}Se and ^{96}Zr nuclei. Their behaviors are very similar, which led us to propose our recipe to set the isoscalar strength. One sees that $s_{sym} = 1.0$, while values of t_{sym} (indicated by points on the axis t) are > 1, and vary with the mass number A. Exactly the same happens for the remaining four nuclei, and their values of s_{sym} and t_{sym} are listed in Table I. The values exhibited for the latter are very close to those obtained previously in [21, Table 4], and in [28, Table 4.9], where Method III was used to calculate the NM. The above similarity is the main reason for associating PSU4SR to isospin symmetry restoration in $\beta\beta$-decay.

In the literature, the isoscalar strength is usually adjusted by employing the measured $\beta\beta_{2\nu}$ half-lives, from which the absolute value of $M^{2\nu}$ can be extracted but not its sign. In doing so, two different values of t are obtained: one ($t = t_\uparrow$) when $M^{2\nu}$ is assumed to be positive ($M^{2\nu} \equiv M^{2\nu}_\uparrow > 0$), and another one ($t = t_\downarrow$) when $M^{2\nu}$ is assumed to be negative ($M^{2\nu} \equiv M^{2\nu}_\downarrow < 0$) . [5] In addition to this disadvantage, it is clear that in this case the model is no longer predictive. We have done such a calculation in Ref. [21] within Method III, finding that in all cases $t_{sym} \approx t_\uparrow$.

Also in Table I, the theoretical energies of F and GT resonances are displayed. They are defined, respectively, as

$$E_{IAS} = \frac{\sum_{pn\alpha} |\rho'^-(pn0^+_\alpha)|^2 \Omega'_{0^+_\alpha}}{\sum_{pn\alpha} |\rho'^-(pn0^+_\alpha)|^2}, \tag{4.1}$$

and

$$E_{GTR} = \left. \frac{\sum_{pn\alpha} |\rho'^-(pn1^+_\alpha)|^2 \Omega'_{1^+_\alpha}}{\sum_{pn\alpha} |\rho'^-(pn1^+_\alpha)|^2} \right|_{\Omega'_{1^+_\alpha} > 10 MeV}, \tag{4.2}$$

where the constraint on GT energies has been imposed since significant GT strength is always observed at low energy far from the location of the GTR. This is particularly so in the case of ^{96}Zr, which causes the calculated energy of the GTR to be relatively low.

It is worth noting that, for $s = s_{sym}$ and $t = t_{sym}$, the total strengths S^+_F and S^+_{GT} not only are minimum, but the concentrations of transition intensities S^-_F and S^-_{GT} in resonant states are also maximum.

The corresponding experimental energies of the IAS are evaluated as

$$E^{Exp}_{IAS} = \mathcal{E}_{Coul}(Z+1, A) - \mathcal{E}_{Coul}(Z, A), \tag{4.3}$$

where (see Eq. (69) in Ref. [5])

$$\mathcal{E}_{Coul}(Z, A) = 0.70 \frac{Z^2}{A^{1/3}} [1 - 0.76 Z^{-2/3}] \text{MeV}. \tag{4.4}$$

The energy difference $E^{Exp}_{GTR} - E^{Exp}_{IAS}$ is estimated from (1.5). A relatively good agreement between the calculations and the experimental estimates indicates that: 1) our choice of the coupling constants in the ph channel is reasonable, and 2) in the closure approximation for the $\beta\beta_{0\nu}$-decay it is proper to replace the intermediate energies $\omega_{J^+_\alpha}$ in (2.23) by an average value $\overline{\omega}_{J^+_\alpha} = 12$ MeV. It should be said, however, that the calculated energies E^{cal}_{IAS} differ appreciably from the "experimental" energies

[5] In our numerical calculations $M^{2\nu}$ is negative at $s = t = 0$, as seen from Figs. 1 and 2. See also Eq. 3.30.

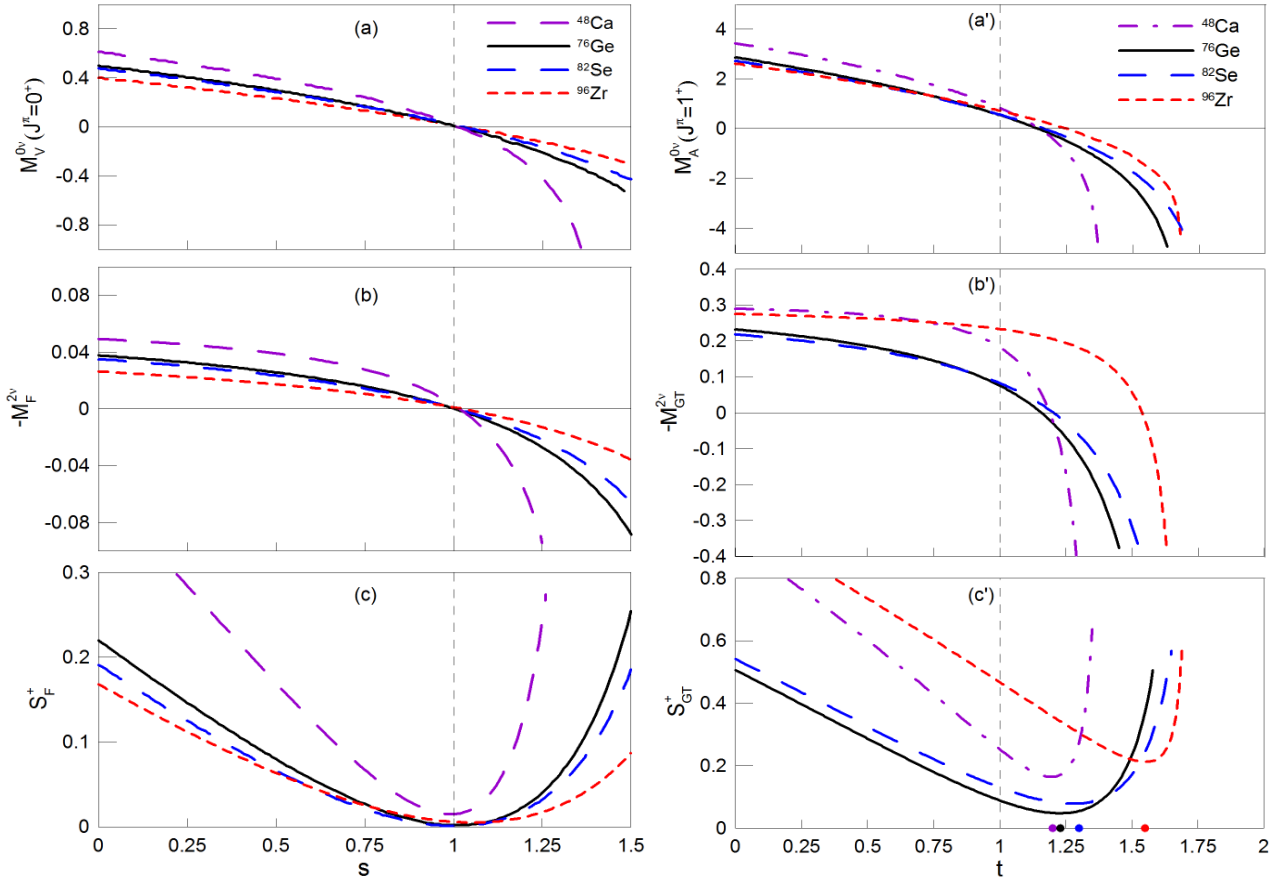

FIG. 1: (Color online) (a) & (a'): 0ν NM normalized to g_A^2 ; (b) & (b'): 2ν NM given in natural units; and (c) & (c'): β^+-decay transition strengths . We show the vector observables, as a function of the ratio $s = v^s_{pp}/\overline{v}^s_{pair}$, on the left side, and axial-vector ones, as a function of the ratio $t = v^t_{pp}/\overline{v}^s_{pair}$, on the right side. The values of t_{sym} on the axis t are indicated by points.

TABLE II: $\beta\beta_{2\nu}$-decay moments evaluated within the BCS (unperturbed) and QRPA (perturbed) approximations are compared with the experimental results $|M^{2\nu}_{exp}|$ recommended by Barabash [3]. All the quantities are given in natural units. As explained in the text, the upper and lower theoretical errors on $M^{2\nu}$ were evaluated with $t = 1.03\times t_{sym}$, and $t = 0.97\times t_{sym}$, respectively, where the values of t_{sym} are those listed in Table I.

	BCS			QRPA			
$^A Z$	$M^{2\nu}_F$	$M^{2\nu}_{GT}$	$M^{2\nu}$	$M^{2\nu}_F$	$M^{2\nu}_{GT}$	$\lvert M^{2\nu}\rvert$	$\lvert M^{2\nu}_{exp}\rvert$
^{48}Ca	-0.148	-0.545	-0.693	-0.004	0.022	$0.018^{+0.110}_{-0.035}$	0.038 ± 0.003
^{76}Ge	-0.193	-0.693	-0.886	-0.000	0.051	$0.051^{+0.035}_{-0.030}$	0.113 ± 0.006
^{82}Se	-0.217	-0.686	-0.903	-0.001	0.062	$0.062^{+0.033}_{-0.029}$	0.083 ± 0.004
^{96}Zr	-0.107	-0.878	-0.985	-0.001	0.024	$0.023^{+0.157}_{-0.036}$	0.080 ± 0.004
^{100}Mo	-0.126	-1.213	-1.339	-0.001	0.035	$0.034^{+0.182}_{-0.115}$	0.185 ± 0.005
^{128}Te	-0.296	-1.174	-1.470	-0.003	0.086	$0.083^{+0.029}_{-0.026}$	0.046 ± 0.006
^{130}Te	-0.263	-1.025	-1.288	-0.002	0.083	$0.081^{+0.022}_{-0.020}$	0.031 ± 0.004
^{150}Nd	-0.057	-0.887	-0.944	-0.001	0.067	$0.067^{+0.011}_{-0.011}$	0.058 ± 0.004

E^{exp}_{IAS} in the case of ^{48}Ca and ^{150}Nd nuclei. The difference between energies E^{cal}_{GTR} and E^{exp}_{GTR} in ^{96}Zr is quite significant also. But, we have not found any satisfactory explanation for these discrepancies.

To appreciate the effect of the residual interaction, and hence of the PSU4SR, we will compare the QRPA with the BCS, which is its mean field approximation in this case. We show our calculated values of the $\beta\beta_{2\nu}$-decay moments in natural units as the corresponding experimental moments, recommended by Barabash [3], are given in these units. Our BCS (unperturbed) and QRPA (perturbed) results are listed in Table II, together with

TABLE III: $\beta\beta_{0\nu}$-decay moments $M_X^{0\nu}$, as well the total moments $M^{0\nu} = \sum_X M_X^{0\nu}$ (normalized to g_A^2, with $g_A = 1.27$), evaluated within the BCS (unperturbed) and QRPA (perturbed) approximations, are shown. In both cases the FNS and SRC effects are included. Same as in Table II, the upper and lower theoretical g on $M^{0\nu}$ were evaluated with $t = 1.03 \times t_{sym}$, and $t = 0.97 \times t_{sym}$, respectively, where the values of t_{sym} are those listed in Table I. At the bottom of the table are shown the ^{76}Ge results: i) without SRC, in the row labeled as ^{76}Ge *, ii) the bare values of moments, *i.e.,* without the FNS and SRC effects, in the row labeled as ^{76}Ge ** , and iii) the moments obtained in Ref. [11] and derived from relations (4.5).

	BCS					QRPA				
$^A Z$	$M_V^{0\nu}$	$M_A^{0\nu}$	$M_P^{0\nu}$	$M_M^{0\nu}$	$M^{0\nu}$	$M_V^{0\nu}$	$M_A^{0\nu}$	$M_P^{0\nu}$	$M_M^{0\nu}$	$M^{0\nu}$
^{48}Ca	1.91	9.10	-1.54	0.49	9.96	0.58	2.57	-0.76	0.33	$2.72^{-0.40}_{+0.32}$
^{76}Ge	2.52	12.35	-2.15	0.71	13.42	0.64	3.02	-0.86	0.40	$3.19^{-0.24}_{+0.46}$
^{82}Se	2.61	12.58	-2.21	0.72	13.70	0.65	2.76	-0.84	0.39	$2.96^{-0.23}_{+0.22}$
^{96}Zr	2.43	12.70	-2.15	0.71	13.70	0.70	1.89	-0.74	0.38	$2.22^{-0.42}_{+0.35}$
^{100}Mo	2.85	15.17	-2.51	0.84	16.35	0.82	2.48	-0.90	0.45	$2.85^{-0.43}_{+0.42}$
^{128}Te	2.78	13.55	-2.13	0.66	14.87	0.84	3.31	-0.97	0.41	$3.59^{-0.19}_{+0.19}$
^{130}Te	2.48	12.12	-1.91	0.60	13.29	0.75	2.81	-0.84	0.36	$3.07^{-0.16}_{+0.16}$
^{150}Nd	2.02	10.94	-1.75	0.57	11.77	0.77	3.95	-0.93	0.37	$4.16^{-0.12}_{+0.11}$
^{76}Ge*	2.54	12.54	-2.21	0.71	13.57	0.65	3.14	-0.90	0.40	3.29
^{76}Ge**	2.90	13.72	-2.55	1.08	15.14	0.85	3.83	-1.11	0.65	4.22
^{76}Ge [11]						1.74	5.48	-1.60	0.29	5.26

the so-called effective moments $|M^{2\nu}_{exp}| = g_A^2 |M^{2\nu}|$ from Ref. [3]. For the axial-vector coupling constant we have used its free nucleon value of $g_A = 1.27$ [36], instead of the quenched value $g_A^{eff} \cong 1$ since: 1) in this way we obtain a better agreement with data, and 2) although g_A^{eff} is often used in the description of simple β-decays, there is no compelling evidence for using it in the $\beta\beta$-decays.

Even though the recipe introduced above to set the parameters in the *pp* channel makes the theory predictive, this does not necessarily mean that the theoretical predictions have to match with the experimental data. But still, it is not possible to completely suppress the well known sensitivity of $M^{2\nu}$ on the parameter t in the neighborhood of t_{sym} [21, 23]. This, in turn, means that a relatively small variation of t causes large variations in $M^{2\nu}$, being particularly pronounced for ^{48}Ca and ^{100}Mo. Here one should keep in mind that ^{48}Ca is a double-closed shell nucleus, while ^{100}Mo has the $Z = 40$ subshell closed. Therefore, the QRPA may not be the fully appropriate model in these two cases.

The above behavior can be seen clearly by appealing to the SMM discussed in the Appendix, where t_{sym} is well defined ($t_{sym} \equiv t_0$) and t_0 depends on the dominant $|pn; 1^+\rangle$ intermediate state. This, however, does not happen in full numerical calculations where t_{sym} depends in a significant way on the mean field, through the pairing coupling $\overline{v}_s^{pair}$, and the single-particle energies (spe). These quantities are determined in a phenomenological way, and, therefore, are not well established [6]. We have assumed that the resulting uncertainties can be quantified by attributing errors of $\pm 3\%$ to t_{sym}. Thus, the upper and lower theoretical errors on $M^{2\nu}$ in Table II were evaluated with $t = 1.03 \times t_{sym}$, and $t = 0.97 \times t_{sym}$, respectively, where the values of t_{sym} are those listed in Table I. It turns out, however, that the value of $|M^{2\nu}_{exp}|$ in ^{76}Ge, ^{128}Te and ^{130}Te fall outside the theoretical errors.

Even if the agreement between theory and data is not as good as one might wish, it is interesting to note that the BCS results differ from $|M^{2\nu}_{exp}|$ in a manner similar to the differences given by the QRPA results. In fact, while $|M^{2\nu}_{exp}|$ are smaller by a factor ranging from 7.2 in ^{100}Mo to 42 in ^{130}Te, the QRPA results are smaller by a factor going from 14.0 in ^{150}Nd to 42.8 in ^{96}Zr. Large differences (roughly of one order of magnitude) between BCS and QRPA moments come from the PSU4SR, which is crucial to make the theory consistent with experimental data. The conservation of the number of particles is, by far, less significant [20]. It is worth noting that, while in the BCS approximation the moments $M_F^{2\nu}$ contribute significantly to the total moments $M^{2\nu}$, in the QRPA approach they can be neglected for all practical purposes. Moreover, given that there are no free parameters in the nuclear model, the agreement between the theory and the data, as seen from the last two columns in Table II, could be considered to be fairly good.

We must take some care when comparing our four $\beta\beta_{0\nu}$-decay moments $M_V^{0\nu}, M_A^{0\nu}, M_P^{0\nu}, M_M^{0\nu}$, with those defined by other groups, since we do not separate the

[6] Only for ^{150}Nd we have used the spe evaluated theoretically within the (DD-ME2) model by Paar *et al.* [52]

TABLE IV: Fine structure of $M^{0\nu}$ moments (normalized to g_A^2, with $g_A = 1.27$) for ^{76}Ge. The contributions of different intermediate-state angular momenta J^π are listed for both parities $\pi = \pm$.

	BCS					QRPA				
J^π	$M_V^{0\nu}$	$M_A^{0\nu}$	$M_P^{0\nu}$	$M_M^{0\nu}$	$M^{0\nu}$	$M_V^{0\nu}$	$M_A^{0\nu}$	$M_P^{0\nu}$	$M_M^{0\nu}$	$M^{0\nu}$
0^+	1.06	0.00	0.00	0.00	1.06	0.02	0.00	0.00	0.00	0.02
1^+	0.00	4.75	-0.48	0.05	4.33	0.00	-0.39	-0.05	0.01	-0.43
2^+	0.36	0.54	0.00	0.05	0.95	0.14	0.24	0.00	0.03	0.40
3^+	0.00	1.01	-0.35	0.06	0.72	0.00	0.45	-0.16	0.03	0.32
4^+	0.14	0.23	0.00	0.04	0.42	0.08	0.14	0.00	0.03	0.24
5^+	0.00	0.40	-0.18	0.04	0.27	0.00	0.24	-0.11	0.03	0.16
6^+	0.06	0.10	0.00	0.03	0.18	0.04	0.07	0.00	0.02	0.13
7^+	0.00	0.15	-0.07	0.02	0.11	0.00	0.11	-0.05	0.02	0.08
8^+	0.02	0.03	0.00	0.01	0.06	0.01	0.02	0.00	0.01	0.05
9^+	0.00	0.06	-0.03	0.01	0.05	0.00	0.04	-0.02	0.01	0.03
10^+	0.00	0.00	0.00	0.00	0.00	0.00	0.00	0.00	0.00	0.00
$\pi = +$	1.64	7.27	-1.11	0.33	8.15	0.29	0.92	-0.39	0.19	1.00
0^-	0.00	0.15	-0.07	0.00	0.08	0.00	0.07	-0.04	0.00	0.03
1^-	0.47	0.62	0.00	0.03	1.12	0.15	0.24	0.00	0.01	0.40
2^-	0.00	2.26	-0.47	0.06	1.85	0.00	0.66	-0.16	0.02	0.52
3^-	0.24	0.43	0.00	0.06	0.72	0.11	0.23	0.00	0.03	0.37
4^-	0.00	0.80	-0.29	0.06	0.57	0.00	0.40	-0.15	0.03	0.28
5^-	0.12	0.21	0.00	0.05	0.38	0.06	0.13	0.00	0.03	0.23
6^-	0.00	0.36	-0.15	0.05	0.26	0.00	0.21	-0.09	0.03	0.15
7^-	0.05	0.10	0.00	0.04	0.19	0.03	0.07	0.00	0.03	0.12
8^-	0.00	0.10	-0.05	0.02	0.08	0.00	0.07	-0.03	0.01	0.05
9^-	0.00	0.01	0.00	0.00	0.02	0.00	0.01	0.00	0.00	0.02
10^-	0.00	0.02	-0.01	0.00	0.01	0.00	0.02	-0.01	0.00	0.01
$\pi = -$	0.88	5.06	-1.04	0.37	5.28	0.35	2.11	-0.48	0.19	2.18

tensor contribution from the GT contribution, nor do we separate $M_P^{0\nu}$ into its PP and AP pieces. For instance, when confronted with the results of Ref. [11] the following correspondence is valid:

$$\begin{aligned} M_V^{0\nu} &\rightarrow M_F^{VV}, \\ M_A^{0\nu} &\rightarrow M_{GT}^{AA}, \\ M_M^{0\nu} &\rightarrow M_{GT}^{MM} + M_T^{MM}, \\ M_P^{0\nu} &\rightarrow M_{GT}^{PP} + M_T^{PP} + M_{GT}^{AP} + M_T^{AP}. \end{aligned} \quad (4.5)$$

The moments labeled as GT and T on the right side are, respectively, the $m = 0$ and $m = 2$ parts of the moments $M_M^{0\nu}$ and M_P in (2.19). This expression also permits an easy visualization of the meaning of moments labeled as AP and PP.

Our four $\beta\beta_{0\nu}$-decay moments and their sums $M^{0\nu}$, evaluated within the BCS (unperturbed) and QRPA (perturbed) approximations are shown in Table III. In both cases, the FNS and SRC effects are included, and the summations over J_α^π in (2.19) go from $J = 0$ to $J = 10$ for both parities. The numerical results are normalized to g_A^2 in order to compare with other calculations.

Some additional results for the 0ν NM in ^{76}Ge are also shown in Table III, namely i) row ^{76}Ge *: without the effect of SRC, ii) row ^{76}Ge **: the bare values, *i.e.,* without the FNS and SRC effects, and iii) row Ref. [11]: results obtained in this paper by Hyvärinen and Suhonen for $g_A = 1.26$, and related to our calculations by means of equations (4.5).

It is worth mentioning that moment $M_V^{0\nu}$ in Ref. [11] is significantly greater than ours, which makes the corresponding total moment $M^{0\nu}$ also much greater than ours. Something similar can be observed from the comparison of the results for most of the other nuclei, as well as when comparing the results of the Refs. [9, 10] with the present results. Moreover, the moments $M^{0\nu}$ in [11] are not always greater than ours, as, for example, is the case of ^{96}Zr. This makes it very difficult to find the reason for the disagreements between different calculations.

The QRPA moments $M^{0\nu}$ are also sensitive to the parameter t in the neighborhood of t_{sym}, although not in such a pronounced way as $M^{2\nu}$. The resulting theoretical QRPA uncertainties, quantified in the way described before, are also shown. These come basically from the uncertainties in $M_A^{0\nu}$, a little bit from $M_P^{0\nu}$ and $M_M^{0\nu}$, and nothing from $M_V^{0\nu}$. Again, the most affected are the

^{48}Ca and ^{100}Mo moments.

The following conclusions can be drawn from the results for the moments $M^{0\nu}$:

i) The role of the residual interaction, through the PSU4SR, is critical in reducing the nuclear moments. The reduction for the neutrinoless decay is, however, less pronounced than in the case of two-neutrino decay, as the perturbed (QRPA) moments $M^{0\nu}$ are only $\sim 5-7$ times smaller than the unperturbed (BCS)moments.

ii) This quenching effect is smaller on induced current moments $M^{0\nu}_P$ and $M^{0\nu}_M$ than on $M^{0\nu}_V$ and $M^{0\nu}_A$, which results from the standard V-A weak current.

iii) Our $M^{0\nu}_M$ are, in principle, larger than in other calculations by the factor $(f_M/g_M)^2 = 1.61$, since we include the term $g_V/2M_N$ in the NRA of the weak Hamiltonian as is usually done in studies of single β-decays. This can be clearly seen from Table III, where all ^{76}Ge moments $M^{0\nu}_X$ from Ref. [11] are higher than ours, except $M^{0\nu}_M$. Note that the differences between both calculations are by far larger than our numerical uncertainties.

iv) Compared to the role played by the residual interaction in the *pp* channel, the FNS and SRC effects are relatively small. Indeed, the FNS effects cause the bare elements to decrease by $\sim 15-20\%$, and when the SRC are added an additional decrease of $\sim 3-5\%$ is produced. These findings are fully consistent with the results exhibited in Table I of Ref. [53], when the SRC are evaluated in the framework of the coupled-cluster method. Moreover, according to the recent studies based on the unitary correlation operator method (UCOM) [54, 55], the SRC have a marginal reduction effect ($< 10\%$) on the $\beta\beta_{0\nu}$-decay moments. Due to this fact, as well as because of computational difficulties, their contributions were omitted directly in a recent paper [35]. Our method to evaluate the SRC, given by (2.28), does not guarantee the correct normalization of the two-body wave function. But, this is a small correction on an effect, which by itself is small, and, therefore, it cannot be relevant.We also note that the effects of the SRC are smaller than our estimate of the theoretical uncertainties.

Fine structure of $M^{0\nu}$ in the case ^{76}Ge is exhibited in Table IV, where contributions of different intermediate-state angular momenta J^π are listed for both parities $\pi = \pm$. Most notable issues in this table are:

1) For $M^{0\nu}_V$, only the natural parity intermediate states $\pi = (-)^J$, *i.e.,* for $J^\pi = 0^+, 1^-, 2^+, \cdots$, contribute.

2) For $M^{0\nu}_P$, only the unnatural parity intermediate states $\pi = -(-)^J$, *i.e.,* for $J^\pi = 0^-, 1^+, 2^-, \cdots$, contribute.

3) The residual interaction in the *pp* channel mainly affects the moment $M^{0\nu}_V$ for $J^\pi = 0^+$ and the moment $M^{0\nu}_A$ for $J^\pi = 1^+$.

4) In the QRPA, the negative parity states dominate the positive parity states.

TABLE V: $M^{2\nu}$ and $M^{0\nu}$ NM within Method II and Method IV, with three different approximations (App) for the parameter t; namely, values obtained from the PSU4SR (t_{sym}) and from $|M^{2\nu}_{exp}|$ ($t_\uparrow$ and $t_\downarrow$). Results from Ref. [11] for $g_A = 1.26$, which should be compared with ours for $t_\downarrow$ when is used the Method II, are also shown.

		Method II			Method IV		
Nuclei	App	t	$M^{2\nu}$	$M^{0\nu}$	t	$M^{2\nu}$	$M^{0\nu}$
^{48}Ca	sym	1.200	0.124	3.66	1.200	0.018	2.72
	$\uparrow$	1.186	0.040	4.08	1.209	0.038	2.64
	$\downarrow$	1.168	-0.039	4.50	1.170	-0.038	2.96
^{76}Ge	sym	1.230	0.052	4.63	1.230	0.051	3.19
	$\uparrow$	1.280	0.113	4.27	1.296	0.113	2.79
	$\downarrow$	1.005	-0.113	5.81	0.887	-0.113	4.79
	Ref. [11]			5.26			
^{82}Se	sym	1.300	0.051	3.35	1.300	0.062	2.96
	$\uparrow$	1.359	0.083	3.08	1.326	0.083	2.81
	$\downarrow$	0.906	-0.083	4.70	1.003	-0.083	4.37
	Ref. [11]			4.69			
^{96}Zr	sym	1.550	0.014	4.89	1.550	0.023	2.22
	$\uparrow$	1.573	0.081	4.60	1.573	0.081	2.04
	$\downarrow$	1.506	-0.080	5.35	1.481	-0.080	2.68
	Ref. [11]			3.14			
^{100}Mo	sym	1.490	0.173	4.45	1.490	0.034	2.85
	$\uparrow$	1.495	0.186	4.39	1.525	0.186	2.48
	$\downarrow$	1.229	-0.185	6.37	1.347	-0.185	3.92
	Ref. [11]			3.90			
^{128}Te	sym	1.410	0.073	3.14	1.410	0.083	3.59
	$\uparrow$	1.354	0.046	3.32	1.351	0.046	3.86
	$\downarrow$	1.119	-0.046	4.04	1.165	-0.046	4.64
	Ref. [11]			4.92			
^{130}Te	sym	1.450	0.119	3.77	1.450	0.081	3.07
	$\uparrow$	1.302	0.031	4.34	1.343	0.031	3.48
	$\downarrow$	1.192	-0.031	4.78	1.175	-0.031	4.07
	Ref. [11]			4.00			
^{150}Nd	sym	1.290	-0.084	4.66	1.290	-0.067	4.16
	$\uparrow$	1.636	0.058	3.71	1.637	0.058	3.10
	$\downarrow$	1.365	-0.058	4.47	1.324	-0.058	4.06

B. Comparison between Methods II and IV

Relevant results for the comparison of the 0ν NM, obtained within the two-QRPA-method (Method II) and the one-QRPA-method (Method IV), are presented in Table V. This is done for both manners of fixing the isoscalar parameter t, *i.e.,* through the PSU4SR (t_{sym}) and from experimental $\beta\beta_{2\nu}$ NM $|M^{2\nu}_{exp}|$ ($t_\uparrow$ and $t_\downarrow$). A few details for ^{76}Ge are shown in Fig. 2, for different approximations for the parameter t. In comparing the results with Methods II and IV, for the same values of t_{sym} that are given in Table I, one notices quite signif-

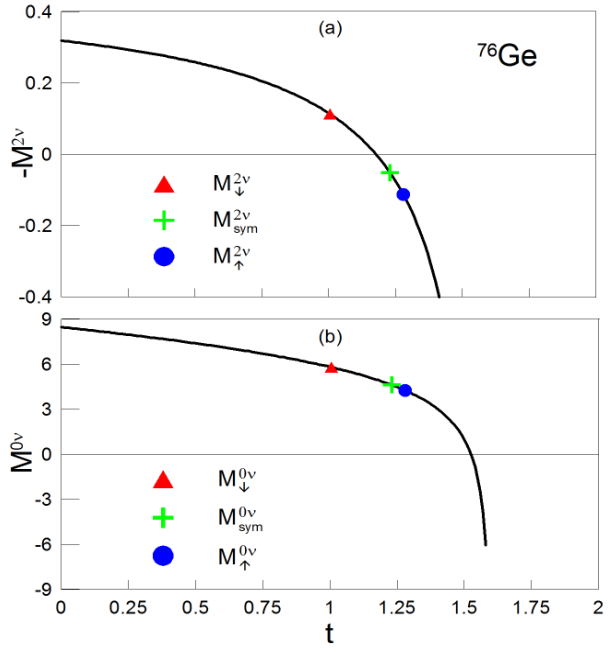

FIG. 2: (Color online) Isoscalar parameters t in ^{76}Ge within the Method II for $|M^{2\nu}_{exp}| = 0.113$. In (a) the NM $M^{2\nu}$ is given in natural units; while in (b) the $M^{0\nu}$ is dimensionless. It should be noted that $M^{2\nu}$ is negative at $t = 0$.

icant differences for both 2ν and 0ν NM. It was to be expected that the 2ν moments differ significantly, since they are very sensitive to t. But, it is somewhat surprising that, except in the case of ^{128}Te, the 0ν moments were appreciably larger using Method II instead of Method IV.

As already observed in Ref. [21], the isoscalar strength can not be determined univocally by adjusting the calculation to the measured half-life, since only the module of $M^{2\nu}_{exp}$ is obtained from experimental data. As a consequence, two values of t result for the calculated NM: one when $M^{2\nu}_{exp}$ is assumed to be positive ($t = t_{\uparrow}$), and one when it is assumed to be negative ($t = t_{\downarrow}$). Due to a smooth variation of calculated $M^{0\nu}$ in the neighborhood where $M^{2\nu}$ passes through zero, the values of $M^{0\nu}_{\uparrow}$ and $M^{0\nu}_{\downarrow}$ are not severely different from each other and in most of the cases $M^{0\nu}_{\uparrow} \sim M^{0\nu}_{sym}$.

The statement quoted above, on the difference in the values of $M^{0\nu}$ obtained for t_{sym} when using Method II or Method IV, attracts attention. To fully convince ourselves of this, we also compare in Table V the results obtained for $M^{0\nu}$ from $t_{\uparrow}$ and $t_{\downarrow}$, arriving at nearly the same conclusion. As both comparisons are consistent, our statement has greater reliability.

To calculate the 0ν moments in the literature $t_{\downarrow}$ is usually chosen, or its equivalent [9, 11], (see, for instance, [56, Fig. 1], and [57, Fig. 6]), even though there is no reason a priori to disregard results obtained with $t_{\uparrow}$. Therefore, it is appropriate to compare the $M^{0\nu}$ values reported in these works for $g_A = 1.27$ and $g_A = 1.26$, respectively, with our $M^{0\nu}_{\downarrow}$. The main difference is that in Refs. [9] and [11], two-nucleon interactions, based on the Bonn one-boson-exchange G matrix, have been used as the residual interaction, instead of the simple δ-force given by (1.2). Despite this important difference, the discrepancy between our results and those of Ref. [11] are not drastically large, as seen in Table V. In fact, the differences between the present results and those from [11, Table III] are of the same order as those between the results in Refs. [9] and [11].

More explicitly, if we proceed in the same way as in Ref. [11] and quantify the differences by the relative differences $(|M^{0\nu}[10] - M^{0\nu}_{\downarrow}|/M^{0\nu}_{\downarrow})$, we get $(9, 0, 41, 38, 22, 16)\%$ for (^{76}Ge, ^{82}Se, ^{96}Zr, ^{100}Mo, ^{128}Te, ^{130}Te), which should be confronted with the differences $(6, 35, 6, 50, 3, 9)\%$, listed in the last column of [11, Table III] for the same set of nuclei. In our calculation the differences go up $\sim 40\%$ in ^{96}Zr and ^{100}Mo because the t value is in the QRPA breakdown region, which is reflected in the theoretical errors shown in Table II.

This behavior of the QRPA is a well-known puzzle in the $\beta\beta_{2\nu}$-decay, and it has not yet been fully disentangled, despite much effort being invested in doing so, through the renormalized QRPA (RQRPA)[23, 58, 59]. However, the results for ^{100}Mo shown in [23, Fig. 3] and [58, Fig. 3] could be considered auspicious, since within the RQRPA the moment $M^{2\nu}$ behaves smoothly in the region of t where the ordinary QRPA collapses.

Rodin *et al.* [60] justify the procedure of fixing t from $\beta\beta_{2\nu}$ data, since in this way the $M^{0\nu}$ values become essentially independent of the size of the single-particle basis. The same thing happens, however, when this parameter is fixed by the PSU4SR procedure. This can be seen, for instance, from Fig. 2 in Ref. [21], where three different single-particle bases for ^{48}Ca have been used in the framework of one-QRPA Method III.

The above authors [60] also argue that: "It follows from the study of Ref. [61] that choosing the negative sign of $|M^{2\nu}_{exp}|$ would lead to a complete disagreement with the systematics of single beta decays." This assertion is based mostly on a work performed within the deformed QRPA [61], where the $\beta\beta_{2\nu}$-decays suppression mechanism is attributed to nuclear deformation. Such a view is obviously in total opposition to ours, in which the decisive player is the restoration of the SU(4) symmetry. In addition, the two-QRPA method is used in [61].

Stating in greater detail: while our model is formulated to describe spherical nuclei, a deformed mean-field is used in Ref. [61], complemented with a schematic spin-isospin separable residual interaction that contains two parts, an attractive ph and a repulsive pp, with coupling strengths χ^{ph} and κ^{pp}, respectively. By performing a detail calculation of the $\beta\beta_{2\nu}$-decay of ^{76}Ge, it is found that: i) the positive value of $|M^{2\nu}_{exp}|$ is reproduced well for $\kappa^{pp}_{\downarrow} = 0.028$ MeV, which was deduced by Homma *et al.*[62] from a systematic study of the single β^+-decays, and ii) the negative value of $|M^{2\nu}_{exp}|$ is disfavored due to a complete disagreement with this study, since a large value for $\kappa^{pp}_{\uparrow}$ ($\cong 0.07 - 0.075$ MeV) is required, that is

above the critical value, $\kappa^{pp} \equiv \kappa_c^{pp} \cong 0.06$ MeV, where the deformed QRPA collapses [62].

This large difference by a factor of ~ 3 between $\kappa_{\uparrow}^{pp}$ and $\kappa_{\downarrow}^{pp}$ should be compared with the small difference of $\sim 25\%$ between t_{sym} and $t_{\downarrow}$, found here for ^{76}Ge. Therefore, we will not necessarily encounter the same difficulties in reproducing simple β-decay with PSU4SR as faced with $\kappa_{\uparrow}^{pp}$ in Ref. [61]. Our preliminary calculations of the GT β^--strength confirm this fact, but detailed study is still necessary.

Finally, we compare the relative differences between the $M^{0\nu}$ obtained with our proposal, *i.e.,* with t_{sym} and Method IV, and with the usual QRPA calculations, based on $t_{\downarrow}$ and Method II. That is, we evaluate the quantity $|M_{sym}^{0\nu}(\mathrm{IV}) - \mathrm{M}_{\downarrow}^{0\nu}(\mathrm{II})|/\mathrm{M}_{\downarrow}^{0\nu}(\mathrm{II})$, from where we get the differences of $(40, 45, 37, 58, 55, 11, 36, 7)\%$ for (^{48}Ca,^{76}Ge, ^{82}Se, ^{96}Zr, ^{100}Mo, ^{128}Te, ^{130}Te,^{150}Nd). Therefore, the cases our procedure leads to smaller matrix elements by $\sim 40\%$ compared with standard evaluations. As seen from Table V this difference basically arises from the one-QRPA-method, employed here instead of the currently used two-QRPA-method. The difference is partially due also to the way of carrying out the restoration of the spin-isospin symmetry.

V. FINAL REMARKS

This study was motivated by the interest shown recently by several groups [9–13] in the relationship between the restoration of $SU(4)$ symmetry and the $\beta\beta$-decay moments, which was addressed by some of the present authors earlier [14–22]. Therefore, we thought it appropriate to update those studies and stress once again the strong bonding between the residual interaction, the GSC, the PSU4SR and the quenching of the $\beta\beta$-decay NM. All this we do in the framework of the QRPA, for which we have provided a review in Sec. III of different approximations used in the literature. In addition, we make a thorough and updated discussion of $\beta\beta_{2\nu}$ moments, and consider contributions of the induced weak currents to the $\beta\beta_{0\nu}$ moments.

From the comparison, done in Tables II and III between the mean field results, described here within the BCS approximation, and the full QRPA calculations using Method IV, it is evident that the residual proton-neutron interaction plays a fundamental role in the PSU4SR, not only in the *pp* channel but also in the *ph* channel. The results shown in Table V testify that this also occurs within the framework of the commonly used Method II, and by adjusting the isoscalar strength to the measured $\beta\beta_{2\nu}$ half-life.

As explained in the previous section, Method IV only involves the nuclei in which the process takes place, while Method II also implies the neighboring nuclei through the GSC. In addition, Method IV is simpler, and, like Method III, allows a discussion of the consequences of

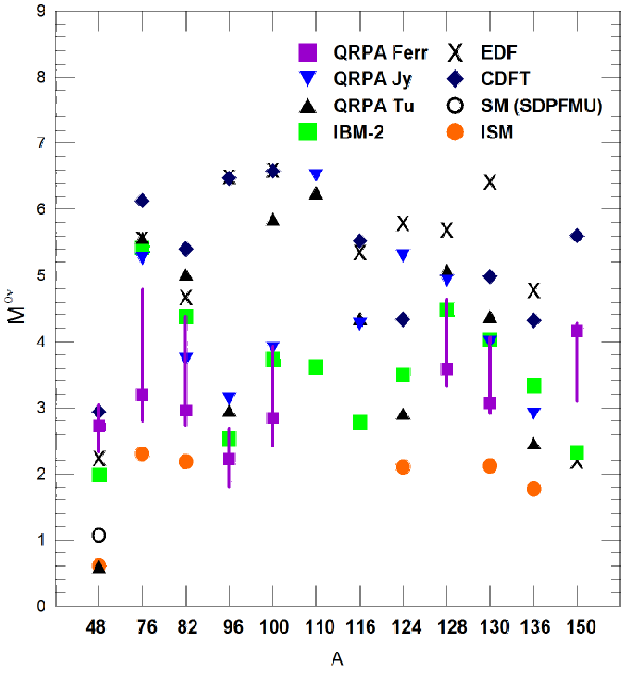

FIG. 3: (Color online) $\beta\beta_{0\nu}$ nuclear moments evaluated with several nuclear structure model calculations: i) QRPA by Tübingen (QRPA Tü) [9] ($g_A = 1.27$), Jyväskylä (QRPA Jy) [11] ($g_A = 1.26$) groups, and our results from Table III (QRPA Ferr) ($g_A = 1.27$), ii) interacting shell model (ISM) [54] ($g_A = 1.25$), Large-scale shell model (SM (SDPFMU)) [63], iii) interacting boson model (IBM-2) [64] ($g_A = 1.269$), vi) energy density functional method (EDF) [65] ($g_A = 1.25$), and covariant density functional theory (CDFT) [35, 66] ($g_A = 1.254$). All results are normalized to g_A^2. The theoretical "errors" presented in our calculations are evaluated as described in the text. The present figure is similar to [35, Fig. 7], [57, Fig. 5][67, Fig. 4], and [68, Fig. 1] .

GSC within the SMM, and the calculation of NM by a simple matrix inversion, without resolving the equation QRPA [15]. Because of all of this, we find that Method IV is preferable to Method II.

Moreover, the above statement on the role of the residual interaction is valid for any other QRPA calculation, as well as for the shell-model evaluations of the charge-exchange matrix elements and resonances. In other words, in all cases the residual interaction in this way quenches the $\beta\beta$-decays mean-field results. Therefore, it is not surprising that all theoretical studies, shown in Fig. 3, yield similar results for $\beta\beta_{0\nu}$ moments, when compared with the mean field results. However, it is worth noting that our results are lower on average by $\sim 40\%$. The theoretical uncertainties in Fig. 3 were increased, relative to 3% used in Table III, in such a way so that they also cover the $M_{\uparrow}^{0\nu}$(IV) and $M_{\downarrow}^{0\nu}$(IV) results of Table V, obtained via fits to the $\beta\beta_{2\nu}$ data.

The SMM presented in the Appendix clearly shows that the PSU4SR within the QRPA is manifested through a very strong cancelation effect between the for-

ward and backward going contributions in the particle-particle channel. Within the Quasiparticle Tamm-Dancoff Approximation [49] and the Shell Model [63], the equivalent quenching effect is induced by the cancelation between seniority zero and seniority four contributions to the $\beta\beta$-moments.

In short, it can be stated that the central achievement of the present work is the realization that PSU4SR, driven by the residual interaction, is the principal actor in shaping the $\beta\beta$-decays, independently of the underlying nuclear model that is used. Being aware of this fact, we have tried to exploit this relevant property of the residual interaction as much as possible. Perhaps it would not be an exaggeration to say that the differences between different theoretical studies are mainly due to the different ways to restore spin-isospin symmetry.

Strictly speaking, the partial SU(4) symmetry restoration is present in all QRPA calculations, since all of them involve a residual interaction. The advantages of performing it via the minima of the β^+-strength over the fit to $\left|\mathcal{M}^{2\nu}_{exp}\right|$, has been disclosed in point 5) in Sec. I. We add here that the proposed recipe to carry out this restoration is based on physically robust arguments, which makes the theory predictive, producing the 2ν moments that are of the same order of magnitude as the experimental ones. This is done without resorting to any free parameter, which is a non-minor achievement, when compared with the mean field results which are one order magnitude larger, and is one more reason for preferring our way of setting the isovector pp parameter instead of the standard form. The agreement with $\beta\beta_{2\nu}$ data is only modest, and it is somewhat disconcerting that the estimates of theoretical uncertainties are greater than the experimental ones. Again, the reason for this is that the t value is in the QRPA breakdown region for $\beta\beta_{2\nu}$ decay. But this is open to further study, and it is possible that in the not too distant future more precise results will be obtained for 2ν-moments.

Moreover, given the widespread use of the $\left|M^{2\nu}_{exp}\right|$ - fitting method, based on the justification that $M^{0\nu}$ and $\mathcal{M}^{2\nu}$ are similar, it is difficult to say which of the two procedures is preferable. To discern between them, it might be useful to simultaneously analyze the single and double GT decays in the framework of the PSU4SR. A step in this direction was given a long time ago by our group [17], which would now have to be updated in the light of recent developments in that direction, such as Refs. [69–73]. In the same sense, it would be interesting to study the first-forbidden beta transitions [74] and their respective giant resonances [75, 76], in the context of SU(4) symmetry.

Acknowledgments

Work partially supported by the Argentinean agency Consejo Nacional de Investigaciones Científicas y Técnicas - CONICET, Grant No.PIP 0377 (F.K.). V. dos S.F. and A.R.S. thank the financial support of FAPESB (Fundação de Amparo à Pesquisa do Estado da Bahia), FAPERJ (Fundação de Amparo à Pesquisa do Estado do Rio de Janeiro) and CAPES-AUXPE-FAPESB-3336/2014/Processo no: 23038.007210/2014-19. We sincerely thank Professor Wayne Seale for his very careful and judicious reading of the manuscript. We also thank N. Paar for providing us with the spe for ^{150}Nd, evaluated within the (DD-ME2) model. One of us is thankful to W. Haxton and J. Engel for stimulating comments and discussions, as well as to the Institute for Nuclear Theory at the University of Washington for the hospitality, and the Department of Energy for partial support.

Appendix: QRPA within the Single Mode Model

In the SMM there is only one intermediate state α and the RPA matrix elements in (3.3) become (see [49, Eqs.(28-31)]):

$$\begin{aligned} A_{J^\pi} &= \omega_0 + [(u_{\rm p}^2 v_{\rm n}^2 + v_{\rm p}^2 u_{\rm n}^2)\mathrm{F}_{J^\pi}(pn) \\ &+ (u_{\rm p}^2 u_{\rm n}^2 + v_{\rm p}^2 v_{\rm n}^2)\mathrm{G}_{J^\pi}(pn)], \\ B_{J^\pi} &= 2v_{\rm p}u_{\rm n}u_{\rm p}v_{\rm n}\left[\mathrm{F}_{J^\pi}(pn) - \mathrm{G}_{J^\pi}(pn)\right]. \end{aligned} \quad (A.1)$$

where

$$\omega_0 = -\frac{1}{4}[\mathrm{G}_{0^+}(pp) + \mathrm{G}_{0^+}(nn)] \quad (A.2)$$

is the unperturbed energy, and $\mathrm{G}_{J^\pi}(pn) = \mathrm{G}(\mathrm{pn,pn;J^\pi})$, *etc.* Moreover, from (3.2) one obtains

$$\begin{aligned} \omega_{J^\pi} &= \sqrt{A^2_{J^\pi} - B^2_{J^\pi}}, \\ X_{J^\pi} &= \frac{A_{J^\pi} + \omega_{J^\pi}}{\sqrt{(A_{J^\pi} + \omega_{J^\pi})^2 - B^2_{J^\pi}}}, \\ Y_{J^\pi} &= \frac{-B_{J^\pi}}{\sqrt{(A_{J^\pi} + \omega_{J^\pi})^2 - B^2_{J^\pi}}}, \end{aligned} \quad (A.3)$$

and

$$\begin{aligned} (X^2_{J^\pi} + Y^2_{J^\pi}) &= \frac{(A_{J^\pi} + \omega_{J^\pi})^2 + B^2_{J^\pi}}{(A_{J^\pi} + \omega_{J^\pi})^2 - B^2_{J^\pi}}, \\ X_{J^\pi}Y_{J^\pi} &= -\frac{(A_{J^\pi} + \omega_{J^\pi})B_{J^\pi}}{(A_{J^\pi} + \omega_{J^\pi})^2 - B^2_{J^\pi}}. \end{aligned} \quad (A.4)$$

This yields

$$\rho_{J^\pi} = \frac{\left[(A_{J^\pi}+\omega_{J^\pi})^2+B_{J^\pi}^2\right]u_{\rm p}v_{\rm n}v_{\rm p}u_{\rm n}-(A_{J^\pi}+\omega_{J^\pi})B_{J^\pi}(u_{\rm p}^2v_{\rm n}^2+v_{\rm p}^2u_{\rm n}^2)}{(A_{J^\pi}+\omega_{J^\pi})^2-B_{J^\pi}^2}. \quad (A.5)$$

Since

$$\begin{aligned}(A_{J^\pi}+\omega_{J^\pi})^2+B_{J^\pi}^2 &= 2A_{J^\pi}(A_{J^\pi}+\omega_{J^\pi}),\\ (A_{J^\pi}+\omega_{J^\pi})^2-B_{J^\pi}^2 &= 2\omega_{J^\pi}(A_{J^\pi}+\omega_{J^\pi}), \quad (A.6)\end{aligned}$$

and employing (A.4) we arrive at a very simple expression

$$\rho_{J^\pi} = \rho_0\frac{\omega_0}{\omega_{J^\pi}}\left(1+\frac{{\rm G}_{J^\pi}}{\omega_0}\right), \quad (A.7)$$

where $\rho_0 = u_{\rm p}v_{\rm n}v_{\rm p}u_{\rm n}$ is the unperturbed BCS two-body particle-hole density matrix. Therefore, the RPA correlations in the SMM, besides modifying the unperturbed energy ω_0 into perturbed energies ω_{J^π}, they introduce the renormalization factors (effective $\beta\beta$-decay charge)

$$\mathcal{E}_{J^\pi} = \frac{\rho_{J^\pi}}{\rho_0} = \frac{\omega_0}{\omega_{J^\pi}}\left(1+\frac{{\rm G}_{J^\pi}}{\omega_0}\right), \quad (A.8)$$

which quench all $\beta\beta_{2\nu}$, and $\beta\beta_{0\nu}$ moments. The factor $(1+{\rm G}_{J^\pi}/\omega_0)$ comes from the interference between the forward and backward going RPA contributions, which are coherent in the *pp* channel and totally out of phase in the particle-hole (*ph*) channel. As a consequence, the *ph* matrix elements ${\rm F}_{J^\pi}(pn)$ do not appear in this factor, with only the *pp* matrix elements ${\rm G}_{J^\pi}(pn)$ surviving. It is worth noting that the above result is valid in general, *i.e.,* , for any type of residual interaction, and not only for (1.2).

Moreover, using the same interaction between identical and nonidentical particles for $J^\pi = 0^+$ one has: ${\rm G}_{0^+}(pp) = {\rm G}_{0^+}(nn) = 2{\rm G}_{0^+}(pn)$, which implies $\omega_0 = -{\rm G}_{0^+}(pp)/2 = -{\rm G}_{0^+}(pn)$, which is the condition for the restoration of the isospin symmetry. For the force described by Eq. (1.2), this condition is expressed as

$$1+\frac{{\rm G}_{0^+}(pn)}{\omega_0} = 1-s, \quad (A.9)$$

and for $s = s_{sym} = 1$ is $\mathcal{F}_{0^+} = 0$. This leads to the condition (see (1.3))

$$S_F^+ = M_F^{2\nu} = M_F^{0\nu}(J^\pi = 0^+) = 0, \quad (A.10)$$

which is well fulfilled in full calculations as shown in Table I. Therefore, the SMM nicely explains the restoration of the isospin symmetry.

The SMM is also appropriate for explaining the maximal restoration of the $SU(4)$ symmetry. In fact,

$$1+\frac{{\rm G}_{1^+}(pn)}{\omega_0} = 1-t/t_0, \quad (A.11)$$

and $\mathcal{E}_{1^+} = 0$ for $t = t_0$, the value of which depends on the *pn* single particle state, and $t_{sym} \equiv t_0$. For instance, the dominant single pair configurations in ^{48}Ca and ^{100}Mo are, respectively, $\left[0f_{7/2}(n)0f_{7/2}(p)\right]_{J^+}$ and $\left[0g_{7/2}(n)0g_{9/2}(p)\right]_{J^+}$, and the corresponding values of t_0 are 21/11 and 27/20 (see Ref. [22]). Keep in mind that the restoration of symmetry $SU(4)$ should lead to relations (1.3) and (1.4), but in no way should it be total, since in this case there would be no $\beta\beta$-decay [12].

Finally, it should be stressed that, at variance with the $\beta\beta$-decay moments, the energies ω_{J^π} in (A.8), as well as E_{IAS} and E_{GTR} given by Eqs. (3.4) and (3.5), do not behave as the factor $(1+{\rm G}_{J^\pi}/\omega_0)$, but strongly depend on the *ph* matrix elements F_{J^π} (see Eqs. (7) and (8) in Ref. [22]).

[1] J. Kramp, D. Habs, R. Kroth, M. Music, J. Schirmer, D. Schwalm and C. Broude, Nuc. Phys. **A474** 412 (1987).
[2] Y. Fukuda *et al.*, Phys. Rev. Lett. **81**, 1562 (1998).
[3] A. S. Barabash, Nucl. Phys. **A935**, 52 (2015). arXiv:1501.05133 [nucl-ex].
[4] D. Tosi on behalf of the EXO Collaboration, arXiv:1402.1170v1 [nucl-ex].
[5] A. Bohr and B.R. Mottelson, *Nuclear Structure* (Benjamin, New York, 1969) vol. 1.
[6] P. Vogel and W. E. Ormand, Phys. Rev. C **47**, 623 (1993).
[7] Yu. S. Lutostansky a, V. N. Tikhonov, JETP Lett. **102**, no.1, 7 (2015), and EPJ Web Conf. **107**, 06004 (2016).
[8] J. Bernabeu, B. Desplanques, J. Navarro, S. Noguera, Z. Phys. C **46** (1990) 323; B. Desplanques, S. Noguera, J. Bernabeu, Z. Phys. C **51** (1991) 499
[9] F. Šimkovic, V. Rodin, A. Faessler, and P. Vogel, Phys. Rev. C **87**, 045501 (2013).
[10] Dong-Liang Fang, A. Faessler, and F.Šimkovic, Phys. Rev. C **92**, 044301 (2015), arXiv:1508.02097.
[11] J. Hyvärinen and J. Suhonen, Phys. Rev. C **91**, 024613 (2015).
[12] D. Stefanik, F. Šimkovic, and A. Faessler, Phys. Rev. C **91**, 064311 (2015), arXiv:1506.00835.
[13] S.Ünlü and N. Çakmak, Nucl. Phys. **A939**, 13 (2015).
[14] F. Krmpotić, in *Lectures on Hadron Physics*, ed. E. Ferreira (World Scientific, Singapore, 1990) 205.
[15] J. Hirsch and F. Krmpotić, Phys. Rev. **C41**, 792 (1990).
[16] J. Hirsch and F. Krmpotić, Phys. Lett. **B246**, 5 (1990).
[17] J. Hirsch, E. Bauer and F. Krmpotić, Nucl. Phys. **A516**,

304 (1990).
[18] F. Krmpotić, J. Hirsch and H. Dias, Nucl. Phys. **A542**, 85 (1992).
[19] F. Krmpotić, Phys. Rev. C **48**, 1452 (1993).
[20] F. Krmpotić, A. Mariano, T.T.S. Kuo and K. Nakayama, Phys. Lett. **B319**, 393 (1993).
[21] F. Krmpotić and S. Shelly Sharma, Nucl. Phys. **A572**, 329 (1994).
[22] F. Krmpotić, Rev. Mex. Fís. **40**, 285 (1994).
[23] F. Krmpotić, T.T.S. Kuo, A. Mariano, E.J.V. de Passos and A.F.R. de Toledo Piza, Nucl. Phys. **A612**, 223 (1997).
[24] C. Barbero, J. M. Cline, F. Krmpotić and D. Tadić, Phys. Lett. **B392**, 419 (1997).
[25] C. Barbero, F. Krmpotić and D. Tadić, Nucl. Phys. **A628**, 170 (1998).
[26] C. Barbero, F. Krmpotić, A. Mariano and D. Tadić, Nucl. Phys. **A650**, 485 (1999).
[27] C. Barbero, F. Krmpotić, A. Mariano and D. Tadić, Phys. Lett. **B445**, 249 (1999).
[28] V. dos S. Ferreira, Dissertação de Mestrado: "Cálculos Teórico-Computacionais para duplo decaimento beta", Universidade Estadual de Santa Cruz, Ilhéus, Bahia-BA, Brazil, (2016).
[29] F. Šimkovic, G. Pantis, J. D. Vergados and A. Faessler, Phys. Rev. C **60**, 055502 (1999).
[30] F. Šimkovic, A. Faessler, V. Rodin, P. Vogel and J. Engel Phys. Rev. C **77**, 045503 (2008).
[31] K. Nakayama, A. Pio Galeão and F. Krmpotić, Phys. Lett. **B114**, 217 (1982).
[32] Yu.V. Gaparov, Yu.S. Lyutostanskii and V.G. Aleksankin, Pisma Zh. Eksp. Teor. Fiz. **34**, 407 (1981).
[33] T. Susuki, Nucl. Phys. **A379**, 110 (1982).
[34] J.D. Walecka, *Theoretical Nuclear and Subnuclear Physics* (Oxford University Press, New York, 1995)
[35] J. M. Yao, L. S. Song, K. Hagino, P. Ring, and J. Meng, Phys. Rev. C **91**, 024316 (2015).
[36] J. Beringer *et al.*(Particle Data Group), Phys. Rev. D **86**, 010001 (2012).
[37] G.E. Brown, S.-O.Backman, E.Oset, and W. Weise Nucl. Phys. A **296**, 191 (1977).
[38] I.S. Towner, Phys. Rep. **155**, 263 (1987).
[39] C. De Conti, F. Krmpotić, B. Vern Carlson, PoS XXXIVBWNP, 126
[40] J. A. Halbleib and R. A. Sorensen, Nucl. Phys. A **98**, 524 (1967).
[41] P. Ring and P. Schuck, *The Nuclear Many-Body Problem*, Springer-Verlang, New York, 1980.
[42] P. Vogel and M. R. Zirnbauer, Phys. Rev. Lett **57**, 3148 (1986).
[43] O. Civitarese, A. Faessler and T. Tomoda, Phys. Lett. B **194**, 11 (1987).
[44] A. Staudt, K. Muto, H.V. Klapdor- Kleingrothaus, Europhys. Lett. **13**, 31 (1990).
[45] L. Pacearescu, A. Faessler and F. Šimkovic, Phys. Atom. Nucl. **67**, 1210 (2004), Yad. Fiz. **67**, 1232 (2004).
[46] M. Saleh Yousef, V. Rodin, A. Faessler and F. Šimkovic, Nucl. Phys. Proc. Suppl. **188**, 56 (2009), and Phys.Rev. C **79**, 014314 (2009).
[47] P. Sarriguren, O. Moreno and E. Moya De Guerra, Adv. High Energy Phys. **2016**, 6391052 (2016).
[48] D. Cha, Phys. Rev. C **27**, 2269 (1983).
[49] F. Krmpotić, Fizika **B14**, 139 (2005).
[50] J. Engel, P. Vogel and M. R. Zirnbauer, Phys. Rev. C **37**, 731 (1988).
[51] T. Tomoda and A. Faessler, Phys. Lett. B **199**, 475 (1987).
[52] N. Paar, P. Ring, T. Nikšić, and D. Vretenar, Phys. Rev. C **67**, 034312 (2003).
[53] F. Šimkovic, A. Faessler, H. Müther, V. Rodin, and M. Stauf, Phys. Rev. C **79**, 055501 (2009).
[54] J. Menéndez, A. Poves, E. Caurier and F. Nowacki, D, Nucl. Phys. A **818**, 139 (2009).
[55] J. Engel and G. Hagen, Phys. Rev. C **79**, 064317 (2009).
[56] V.A. Rodin, A. Faessler, F. Šimkovic, and P. Vogel Phys. Rev. C **68**, 044302 (2003).
[57] J. Engel and J. Menéndez, Rept. Prog. Phys. **80**, 046301 (2017), and arXiv:1610.06548.
[58] J. Toivanen and J. Suhonen, Phys. Rev. Lett. **75** (1995) 410.
[59] V. Rodin and A. Faessler, Phys.Rev. C **66** (2002) 051303; L. Pacearescu, V. Rodin, F. Šimkovic and A. Faessler, Phys.Rev. C**68** (2003) 064310, Phys.Rev. C**75** (2007) 059902(E).
[60] V.A. Rodin, A. Faessler, F. Šimkovic, and P. Vogel, Nucl. Phys. **A766** (2006) 107, Erratum: Nucl. Phys. **A793** (2007) 213.
[61] F. Šimkovic, L. Pacearescu, A. Faessler, Nucl. Phys. **A733** (2004) 321.
[62] H. Homma, E. Bender, M. Hirsch, K. Muto, H.V. Klapdor-Kleingrothaus, T. Oda, Phys.Rev. C**54** (1996), 2972.
[63] Y. Iwata, N. Shimizu, T. Otsuka, Y. Utsuno, J. Menéndez, M. Honma, T. Abe, Phys. Rev. Lett. **116**, 112502 (2016) .
[64] J. Barea, J. Kotila and F. Iachello, Phys. Rev. C **87**, 014315 (2013).
[65] N. L. Vaquero, T. R. Rodríguez and J. L. Egido, Phys. Rev. Lett. **111**, 142501 (2013).
[66] L.S. Song, J.M. Yao, P. Ring, J. Meng, Phys. Rev. C **90**, 054309 (2014).
[67] J.J. Gómez-Cadenas, and J. Martín-Albo, PoS **GSSI14**, 004 (2015).
[68] J. Menéndez, arXiv:1605.05059.
[69] R. Madey, B. S. Flanders, B. D. Anderson, A. R. Baldwin, J. W. Watson, S. M. Austin, C. C. Foster, H. V. Klapdor, and K. Grotz, Phys. Rev. C **40** (1989), 540.
[70] R. L. Helmer, M. A. Punyasena, R. Abegg, W. P. Alford, A. Celler, S. El-Kateb, J. Engel, D. Frekers, R. S. Henderson, K. P. Jackson, S. Long, C. A. Miller, W. C. Olsen, B. M. Spicer, A. Trudel, and M. C. Vetterli, Phys. Rev. C **55** (1997), 2802 .
[71] D. Frekers, *et al.*, Phys. Rev. C **94** (2016), 014614.
[72] P. Sarriguren, O. Moreno and E. Moya De Guerra, Adv.High Energy Phys. **2016** (2016), 6391052.
[73] D.S. Delion and J. Suhonen, Phys. Rev. C **95** (2017), 034330, and references therein.
[74] D. Frekers, M. Alanssari, H. Ejiri, M. Holl, A. Poves and J. Suhonen, Phys. Rev. C **95** (2017), 034619.
[75] F. Krmpotić, K. Ebert, W. Wild, Nucl.Phys. **A342** (1980) 497.
[76] F. Krmpotić, K. Nakayama and A. Pio Galeão, Nucl.Phys. **A399** (1983) 478.